DEFORMATION PROCESSES IN FORGING CERAMICS

Summary Report

June 1969 - August 1970

Prepared for

Office of Advanced Research and Technology
National Aeronautics and Space Administration
Headquarters
Washington, D.C.

Contract NASW-1914

AVSD-0619-70-CR

by

R.M. Cannon
W.H. Rhodes

Approved by

T. Vasilos

T. Vasilos

AVCO CORPORATION
Systems Division
Lowell, Massachusetts 01851

FOREWORD

This work is being performed under the sponsorship of the NASA Headquarters, Office of Advanced Research and Technology, Research Division with Mr. J.J. Gangler as Project Monitor under Contract NASW-1914.

The work is being performed at the Avco Corporation, Systems Division, Lowell, Massachusetts, in the Materials Sciences Department which is under the direction of Dr. T. Vasilos. Mr. R.M. Cannon is principal investigator and is being assisted by Dr. W.H. Rhodes. The authors wish to acknowledge the assistance of Mr. B. MacAllister, in mechanical testing, the microscopy of Messrs. P.L. Burnett, C.L. Houck and R.E. Gardner, and the x-ray diffraction analysis of Mr. P.L. Berneburg and Dr. R.M. Haag. Finally, the discussions and comments of Dr. R.J. Hill and Prof. A.H. Heuer of Case-Western Reserve University are appreciated.

ABSTRACT

The program objective is to investigate the deformation processes involved in forging of polycrystalline oxide ceramics. A combination of mechanical testing and forging experiments were preformed on fine-grained Al_2O_3.

The combination of mechanical tests and microstructural evaluation indicated that at very fine grain sizes the deformation mechanism occurs by a non-Newtonian grain boundary sliding process. In addition, considerable evidence was found for a substantial contribution of basal slip to the grain shape accommodation process. Preferential crack formation was found at inhomogeneities in the specimens; the appearance and growth of these cracks was more rapid at higher strain rates and stresses.

The results of several forgings combined with the mechanical tests support the view that there is sufficient ductility in fine-grained Al_2O_3 to to allow forging at moderate temperatures.

TABLE OF CONTENTS

ABSTRACT

I. INTRODUCTION. 1

II. TECHNICAL APPROACH. 3

A. Problem Areas 3

B. High Temperature Mechanical Behavior. 5

C. Areas for Investigation 12

III. RESULTS 15

A. Mechanical Tests. 15

1. Multiple Bend Tests 15

2. Strain Rate-Grain Size Dependence 23

3. Fracture Stress-Strain Rate Dependence. 30

B. Forging Experiments 32

C. Microstructural Evaluation. 34

1. Deformation Features. 34

2. Cavitation and Cracking 43

3. Crystallographic Texture. 47

IV. DISCUSSION. 50

V. SUMMARY AND CONCLUSIONS 55

VI. APPENDIX - Analysis of Flexural Test Data 57

A. Stress Distribution in the Beam 57

B. Bending Moment Determination. 58

C. Determination of Strain and Strain Rate 62

VII. REFERENCES. 65

LIST OF FIGURES

Figure No.		
1	Apparent Stress Versus Strain Curve for Specimen FLUX-30 Tested at 1450°C.	17
2	Apparent Stress Versus Strain Relations for Multiple Bend Tests.	19
3	Evidence of Strain Enhanced Grain Growth.	20
4	Crack Seen in Surface of Specimen FLUX-30 During Multiple Bending.	22
5	Stress-Strain Rate Curves for the Fine-Grained, Hot Pressed Material C126C.	24
6	Stress-Strain Rate Curves for the Sintered Material	25
7	Strain Rate Versus 1/T Showing the Activation Energy for Deformation	27
8	Dependence of the Activation Energy for Deformation on Grain Size	28
9	Plot of the Strain Rate Dependence on Grain Size.	29
10	Effect of Strain Rate on the Fracture Stress of Fine-Grained Al_2O_3 at 1415°C	31
11	Small Cracks Seen in the Side of Specimen JC-1474 After Forging to 38% Height Reduction	33
12	Top and Bottom Views of Deep Drawn Hemisphere, D-1442 of Al_2O_3.	35
13	Compressive and Tensile Surfaces After the 1st and 2nd Cycles, Respectively, for Specimen FLUX-33.	37
14	Compressive and Tensile Surfaces After the 6th Cycle for Specimen FLUX-33.	38
15	Surface Replicas Showing Distorted Boundaries and Triple Grain Junctions.	39
16	Polished and Etched Sections from Specimen FLUX-30 Showing Distorted Boundaries and Triple Junctions	40
17	Microstructures Showing Deformation Features in Samples JC-1469 and JC-1474 Forged to 16% and 38% Reduction at 1450°C	41

LIST OF FIGURES (Concl'd)

Figure No.		
18	Cross-Section of Specimen JC-1474, Forged to 38% Reduction, Showing Microstructural Texture.	42
19	Fine Surface Steps Seen Primarily on Compression Surfaces which are Suggestive of Fine Slip Bands. . . .	44
20	Protrusion at a Grain Face Extending into a Neighboring Grain	45
21	Microstructure from Specimen JC-1469 Showing Faint Lines and Pits which are Thought to be Traces of a Dislocation Network	45
22	Microstructure of Specimen FLUX-30 Showing a Region with a High Density of Grain Boundary Cavities.	46
23	Intergranular Cracking in Specimen FLUX-32, After Four Bend Cycles	46
24	Ratio of Relative X-ray Intensity for Specimen JC-1474 Forged 39% Showing Basal Texture.	48
25	Temperature Dependence of Yield Stress (at $\dot{\epsilon} = 4 \times 10^{-5}$ sec^{-1}) for 2 μ and 13 μ Polycrystalline Al_2O_3 and for Sapphire Oriented for Basal Slip, Rhombohedral Slip and Basal Kinking	51
A1	Schematic of Curved Bend Bar Showing Relevant Geometry.	60

LIST OF TABLES

A1	Effect of Curvature on the Bending Moment	64

I. INTRODUCTION

There have been several investigations into the hot working of crystalline ceramic oxides in the last several years. Although several of these have been moderately successful, there are still significant problems, which result in part from limitations in the understanding of the high temperature deformation and fracture of the oxides. It is the objective of this program to investigate the forging of several refractory polycrystalline oxides, in order to provide a greater capability in the deformation processing of them. Therefore, the particular objectives of the program can be stated briefly as follows:

1) Understanding of the deformation and fracture behavior necessary for forging polycrystalline ceramic oxides,

2) Successful forging of flaw-free bodies with useful properties,

3) The possible development of unique or otherwise difficult to obtain properties as the result of hot working.

Hot forging, extrusion and rolling have been utilized to date by several investigators.* Successful extrusions of several oxides have been made by Hunt and co-workers at Nuclear Metals and with Rice of Boeing. Although crack-free extrusion of MgO and other relatively ductile oxides have been obtained, the high strain rates and rapid cooling rate are problems and have contributed, in part, to the failure to obtain sound extrusions of the less ductile materials such as Al_2O_3. Vasilos and co-workers[2] at Avco have demonstrated the successful upset forging (press forging) of many refractory oxides, including several, such as Al_2O_3, which have not been successfully extruded. Promising results have also been obtained in shape forging of Al_2O_3.[3] Hot rolling has been more limited although some success has been obtained in the densification of MgO powder[4] and with materials containing a glassy phase.[5] In addition, the extrusion of refractory carbides has been accomplished by Dolloff and Probst,[6] and by Accary et al.[7]

The results of the initial efforts have been encouraging and have indicated that hot working should provide an extension of present forming capabilities and also can provide improved properties in the refractory oxides. Property improvements can be reasonably expected in a number of areas as a result of high density, microstructural and crystallographic texture and perhaps retained dislocation substructure. Moderate increases in strength resulting from extrusion of MgO[1] and upset forging of Al_2O_3[3] have been demonstrated. Upset forging has been used to obtain theoretical density resulting in transparency in a number of oxides.[2] Crystallographic texture from forging results in transparency in Al_2O_3[8] and in high values of magnetic permeability in barium ferrites.[9] Although results of this type are encouraging, significant problem areas such as limited ductility and inadequate microstructural control, require solutions in order to make hot working more feasible.

---

* Good reviews of efforts in the hot working of ceramics can be found in the articles by R.W. Rice.[1]

The approach of this program is to perform controlled forging experiments on oxides and to evaluate the results in terms of the fundamental mechanical properties of these materials. These results are then to be used together with appropriate metalworking techniques to indicate the preferred forging techniques for the oxides and to indicate the effects of starting materials on forgability. Attention is also being given to developing or maintaining desirable microstructures and properties in the forged bodies. Although existing information and data on the deformation and fracture of ceramics is utilized where it exists, the available information on deformation at high strains and on high temperature fracture is rather incomplete. Therefore, basic mechanical testing is required in conjunction with the actual forging. The initial emphasis has been on mechanical testing using the results of previous forging efforts to indicate the necessary areas of investigation.

The primary effort is to be with Al_2O_3 and MgO since these are available in high quality bodies and there is considerable experience in fabricating them, and comparative base-line information is available on properties and microstructures resulting from conventional fabrication techniques. Limited consideration will be given to $MgAl_2O_4$ (spinel) and other compositions in the MgO-Al_2O_3 system to provide information about mixed oxides and multi-phase systems.

The work done during the first year was entirely with Al_2O_3. Extensive mechanical testing has been done in the temperature range of 1250-1750°C in order to provide additional insight concerning the deformation mechanisms and useful data on the yield stress and fracture stress. Tests have been done to evaluate the effects of temperature, strain, strain rate and grain size on flow and fracture. The test results have been coupled with microstructural examination to provide mechanistic insights. In addition, a few forgings were done to provide correlation with the testing and evaluation of some of the forging techniques to be used. Both simple upset forgings and deep drawing of hemispheres were done.

II. TECHNICAL APPROACH

Much of the work to date on the hot working of ceramic oxides has necessarily been of an empirical nature. Although results have been encouraging, there has by now been enough work done to indicate problem areas which must be given basic consideration in order to allow a more sophisticated approach to deformation processing of oxides and to the development of desired properties. The most critical areas have been identified and are discussed briefly; this is followed by a discussion of the various deformation modes which have been identified as important in polycrystalline ceramics. Finally, there is an outline of the basic approach to be used in the program and an indication of the areas of investigation which are considered to be the most promising.

A. Problem Areas

Most of the critical problems can be divided into three broad areas for consideration. The first, and most serious, is the problem of hot tearing, cracking and cavitation. The second area for consideration is the rather broad one of microstructural control resulting from grain growth, strain induced boundary migration and recrystallization. The third area includes the engineering and equipment problems associated with high temperature processing including chemical compatibility, tooling design, lubrication and temperature control.

The problems of limited formability, high rejection rates and microstructural degradation from flaws and cracks have been particularly severe in hot working to date. The application of basic metal working technology is hampered by incomplete understanding of the flow and fracture mechanisms and of reliable data on the properties of particular oxides. The use of analytical treatments of various forging problems is desirable in order to determine limiting conditions of stress or strain and to determine useful modifications. The use of these analytical techniques requires constituitive flow relations and quantified fracture criteria. Such information is not presently available for the ceramic oxides for the conditions of interest; further, there frequently does not exist satisfactory mechanistic understanding of behavior to allow sound qualitative judgements about some of these problems.

Although basic deformation mechanisms have been identified for the oxides, there is still considerable controversey concerning the relative importance of various of them over broad ranges of temperature, stress and strain. Much of the work has been done at low strains and the behavior at higher strains has been generalized from this without adequate characterization or justification. For the particular materials of interest, it is necessary to provide more data on the effect of microstructural variables and test variables on the flow stress-strain relations.

The high temperature fracture of ceramics has received less attention than yielding behavior. Although fracture associated with limited ductility involving failure to satisfy the von Mises condition, requiring five active slip systems, has been observed, the broad conditions for which this condition dominates are not yet clear, especially for Al_2O_3. Intergranular cracking has been frequently observed under conditions where the problem of

insufficient slip systems was not thought to be dominating. Although the obvious embrittlement resulting from weak or low temperature impurity phases has been frequently identified, the effects of smaller amounts of impurities within the nominal solubility limits are not known. The result is that some of the potential failure mechanisms have been identified; however, there does not yet exist a broad understanding of failure in ceramic oxides which would include quantitative fracture criteria relating the variables of temperature, stress, strain and strain rate to microstructural variables.

The type of information which must be made available for application to forging problems includes definition of the conditions under which ductility is too limited to be useful, understanding of the cause and prevention of grain boundary cracking and cavitation which result in eventual hot tearing of the material, determination of rates of strain hardening and the effect on neck resistance and fracture, and finally the effectiveness of high strain rate sensitivity in providing resistance to necking or crack propagation.

Grain boundary cavitation appears to be one of the most serious difficulties. Examples have been seen at Avco in the shape forging of cones and hemispheres of Al_2O_3 where intergranular separation lowered the density from nearly theoretical to as low as 60-65%, but caused only very limited macroscopic tearing; other forging of similar pieces under nominally similar conditions resulted in no loss of density.[3] The causes for the differences are not known, but cannot be simply written off to lack of ductility. This problem is particularly severe in that small amounts of intergranular cracking may be quite deleterious to the low temperature properties.

The entire area of microstructural control during and after deformation processing of ceramic oxides has not been adequately characterized. Forging and extrusion of single crystals of MgO and CaO has resulted in recrystallization to form polycrystalline materials.[1] In addition, both recrystallized and unrecrystallized Al2O3 have been produced by upset forging;[10] the unrecrystallized material having retained dislocation networks and twins.[2] In addition, effects such as polygonization[11], recovery and apparent strain aging[12] have been observed in tensile studies of MgO. Therefore, it should be possible to obtain a wide variety of resultant microstructures and properties. There is, however, relatively little information concerning the exact conditions under which these various phenomena occur and frequently reliable predictions whether or not recrystallization will occur cannot be made.

The problem of retention of extremely fine grain sizes is particularly bothersome because of grain growth at the high temperatures necessary for adequate ductility, this is aggravated by the fact that concurrent straining may enhance growth rates, particularly at low strain rates.[13] This has been a problem in both upset forged Al2O3[2] and extruded MgO[1] in which grain sizes have not been obtained as fine as can be produced by hot pressing. Because of the highly desirable properties associated with fine grained ceramics, this problem requires serious attention. Both recrystallization with grain refinement and lower temperature forging to produce unrecrystallized, fine grained materials are being considered.

The engineering problems associated with forging are not expected to be limiting, although they require continued attention. Graphite tooling and modified hot pressing equipment are largely used; this imposes some restriction on the available pressures which can be utilized; however, alternative solutions are expensive. The most serious limitation is probably that of chemical reaction; however, techniques and separating media have been developed in hot pressing which are useful; variations in these can also result in some control over the die face friction. Tool design is, of course, a significant area and techniques from metal working technology are being utilized to optimize tool design; this is an area where feedback between analysis of forging experiments and mechanical test data can be particularly valuable but reliable constituitive equations are necessary for effective analysis.

B. High Temperature Mechanical Behavior

An extensive review of the literature on deformation of ceramic oxides was undertaken with the objective of identifying the deformation modes and conditions which provide the greatest amount of useful ductility and to gain as much information about high temperature fracture mechanisms as possible; a brief summary is presented here. It is the objective of this program to work with polycrystalline material so that discussion of single crystals has been restricted to that which provides insight into the behavior of polycrystalline bodies. The refractory oxides (polycrystalline) display very limited, if any, ductility at temperatures below 1/3 to 1/2 of the melting point so that the effects of thermal activation, including relatively rapid diffusion, with the resultant time dependence and microstructural instability must be considered with regard to basic mechanisms and resultant microstructures and properties.

The discussion is presented in terms of the various deformation mechanisms of interest; however, both deformation per se and the implications with regard to fracture mode are considered. This is followed by an enumeration of the particular areas which seem most fruitful for investigation in this program.

It seems reasonable to categorize the observed deformation behavior in terms of three distinct mechanisms which may be dominant under appropriate conditions. The approach risks oversimplification in that a combination of or transition between these mechanisms is frequently observed and often a clear identification of the relative importance of them is not possible at the present time. These are crystallographic slip, diffusional creep and a process perhaps best identified as grain boundary sliding (GBS) which may include a range of particular variations, but is extensively observed in fine grained materials.

Deformation by slip has been observed in virtually all of the refractory oxides under appropriate conditions and in some cases at relatively low temperatures. However, most of these materials do not satisfy the Mises criteria requiring five operative, independent slip systems for fully ductile behavior in polycrystalline bodies[14] except under rather limited conditions. If this condition is not met, stress concentrations develop, especially at grain boundaries and cause microcracks which rapidly lead to fracture. Forging under these conditions will not be fruitful and it is

important, therefore, to identify and consider only those conditions under which the Mises requirement is met. It should be emphasized that cracking at grain boundaries can result from a number of other mechanisms including impurity effects as well as other causes of stress concentration[15] and is not per se the result of failure to satisfy the Mises condition.

Deformation by slip has been studied the most extensively in MgO. The resolved critical shear stresses are low enough to allow slip on both the $\{110\}\ [1\bar{1}0]$ and $\{001\}\ [1\bar{1}0]$ slip systems, both of which are necessary for five independent slip systems, and also, to allow cross slip at temperatures as low as 800-1000°C.[12] However, interpenetration of oblique slip bands is difficult below 1700°C, although reduced strain rates lower this to at least 1550°C.[16] The result is fully ductile behavior in polycrystalline MgO cannot be obtained in tension below about 1700°C.[11] At least limited ductility without cracking is possible in some cases as low as 800°C in compression.[12] This difference is thought to result from a reduced tendency for crack propagation rather than from a fundamental difference in deformation mode.

At about 1400°C and above, some grain boundary sliding also occurs which probably does not contribute significantly to deformation in coarse-grained material where slip is predominant; it can, however, provide mechanisms for fracture leading to limited ductility at these intermediate temperatures. This behavior is very similar to that found in many metals at intermediate temperatures.[17] Cracks develop at points of stress concentration, particularly triple points, which lead to intergranular failure.[11,12] In addition, pores develop along grain faces normal to the tensile axis which can eventually interconnect and lead to failure.[11,18] In general, it is expected that the triple point cracking will occur at higher stresses and strain rates and that cavitation along the boundaries will be predominant at lower rates.[15,17] At higher temperatures increased grain boundary migration and lower yield stresses allow increased stress relaxation at triple points and prevent cavitation and cracking at boundaries; when this occurs fully ductile behavior obtains which allows high elongation. Under these conditions MgO is reported to have sufficient work hardening to provide neck stability for elongations in excess of 100%.[16] At these high temperatures fine grain sizes are not generally stable and relatively coarse grained materials result.

The temperatures at which fully ductile behavior results has been reported at 1700-1800°C for MgO with high purity, pore free boundaries which was prepared from recrystallized single crystals.[11] However, for hot pressed materials this temperature is apparently 2200°C or above.[11] This results from residual porosity and impurities. Both of these factors are thought to reduce grain boundary strength and to inhibit migration; in addition, impurities may raise the yield stress for slip making stress relaxation and conformity more difficult. The impurity effects are thought to result from gaseous species not eliminated in hot pressing,[1] from low strength or low melting point constituents such as recently reported for weakening due to retained LiF in CaO,[19] and from the segregation of solute which is known to impede boundary migration.[20] It is interesting to note that this effect of impurities on grain boundary sliding and cracking is very similar to that observed in Al alloys.[17]

Although this behavior has only been extensively studied in MgO, other cubic materials such as CaO, ZrO_2, UO_2 and $MgAl_2O_4$ apparently behave similarly. Extensive tensile ductility has not been reported presumably because of material limitations resulting from porosity and impurities. Compressive studies of hot pressed $MgAl_2O_4$ indicate behavior similar to that of hot pressed MgO in that multiple slip resulted but only small strains were obtained as a result of cracking which was frequently intergranular and apparently associated with some GBS.[21] The creep behavior of ThO_2 and UO_2 appears to be controlled by slip mechanisms under some conditions,[22] and the critical resolved shear stresses for the necessary slip systems in UO_2 are apparently low enough to be activated and correlate reasonably well with yield stresses in polycrystalline material.[23] Materials from this group have been extruded successfully in a similar manner to MgO.[1]

For the non-cubic materials extensive deformation by slip is much more difficult as a result of the limited slip systems which can be easily activated. However, in compression at 1800°C and above, deformation of both Al_2O_3,[2,10] and BeO[21] apparently involves extensive slip. There is still uncertainty concerning the active non-basal slip systems in these materials; it is certain, however, that the non-basal systems have much higher yield stresses and are much more difficult to operate than the basal systems. There is no information on the behavior of these materials in tension under similar conditions; however, problems with limited ductility from slip band interaction and GBS, as found in MgO, must be anticipated. These considerations all suggest that temperatures very near the melting point are necessary to obtain extensive deformation from slip particularly in tension.

Although it is known to occur, there is little information on the contribution to deformation from twinning in polycrystalline oxides. By analogy with hexagonal metals, where it is frequently observed, twinning may be expected to contribute somewhat to the deformation of non-cubic oxides particularly in providing an alternative to non-basal slip. Twinning has been seen in both coarse and fine-grained Al_2O_3,[2-a,25] which is not surprising in view of its frequent observation in sapphire under compression [26] and its occurrence in Al_2O_3 bicrystals in compression.[27] Although twin-twin and twin-grain boundary interactions have been shown to provide fracture nucleation, it is not known whether it is extensive enough in polycrystalline materials to affect macroscopic flow parameters or ductility.

It may also be suggested that deformation could occur in a material without five independent slip systems by a diffusional process providing the additional degree of freedom. Such a mechanism has been postulated which assumed that dislocation climb provides strain in the necesary direction.[28] It could similarly be imagined that diffusional creep may also operate in this way. There is, however, little direct evidence for this type of behavior in polycrystalline ceramics.

Under conditions in which slip apparently did not or could not occur to a significant extent, the deformation of several oxides has been attributed to diffusional creep. In the case of Al_2O_3[29,30] and BeO[31], where slip is difficult, deformation has been observed to approximately fit the relation predicted by Herring[32] of:

$$\dot{\epsilon} = \frac{13.3\ D\Omega\sigma}{kTG^2} \qquad (1)$$

where $\dot{\epsilon}$ and σ are stress and strain rate; D is the diffusivity, G, the grain size and Ω, the volume of the diffusing species, and kT has the usual meaning. There is, however, some uncertainty regarding the diffusing species which is limiting and in some cases calculated values of D are much higher than measured self-diffusivities.[25]

The above model is based on the assumption that lattice diffusion is rate controlling. A similar relation has been developed by Coble for the case where grain boundary diffusion is sufficiently rapid that it is controlling[33]:

$$\dot{\epsilon} = \frac{47.1\ w\ D_b\Omega\sigma}{kTG^3} \qquad (2)$$

where w D_b is the product of the grain boundary width and diffusivity. Most of the oxide data seem to fit the lattice diffusion model better. Analysis of the data, however, indicates that under some conditions the strain rate-grain size exponent is nearly 2.5 in Al_2O_3,[25,29] MgO[18] and BeO[31]; this may be indicative of a contribution from grain boundary diffusion under the appropriate conditions. Observation of diffusional creep has generally been at temperatures and strain rates which are too low to activate slip; the mechanism is expected to become more favorable relative to slip at finer grain sizes because of the strong inverse dependence.

The observations of diffusional creep have invariably indicated concurrent GBS which is as expected in view of the necessity of boundary relaxation for the mechanism to operate.[34] Materials deforming under conditions which were thought to be diffusional creep have generally shown rather limited ductility with the onset of accelerated creep rates occurring after only a few percent strain. Examination has indicated extensive intergranular cracking which has been attributed to the GBS. There have been no detailed studies of this aspect of this deformation mode, but it is likely that grain boundary porosity and impurities aggrevate the problem although cracking has been observed in materials of supposed high purity and density.

Under analogous conditions of strain rate, temperature and grain size somewhat similar deformation has been reported for MgO,[18] UO_2,[35] and ThO_2[36]. The situation is not as clear since agreement of the results with Eq. (1) has generally not been as good as with Al_2O_3 and BeO, and some microstructural evidence of GBS and some slip is generally observed. This is not surprising in view of the greater ease with which slip occurs in these materials. In creep work a transition in behavior between high and low stress has been found in ThO_2,[22] UO_2,[22,37] and MgO[18,38]. This has been interpreted as a shift in mechanism from a slip controlled one such as dislocation climb at high stress to a deformation mechanism which has a nearly linear strain rate sensitivity at low stresses. Interpretation of this low stress mechanism is not clear, but there is some evidence to indicate it may be diffusional creep. As a result, it is not certain whether pure diffusional creep will occur in these materials, but if so, it will be most likely at very low strain rates and stresses where slip is relatively less likely.

At finer grain sizes the deviation in behavior from that predicted by Equations (1) or (2) becomes increasingly more pronounced in both cubic and non-cubic oxides. Similar observations, which include non-linear stress-strain rate behavior, microstructural observations and disagreement of apparent diffusion coefficients, have been made for several materials with grain sizes between 1 and 10 μ, the indication is that the predominant mechanism is neither slip as seen in coarser materials nor diffusional creep, but that it is controlled by GBS. There is not yet good agreement on the basic mechanisms involved, and there are undoubtedly some variations in different materials. Sliding, of course, cannot proceed without grain shape change, so in this context GBS, as a deformation mechanism, is taken here to imply both the boundary sliding per se and the concommittant accommodation process.

As previously mentioned, GBS has been frequently observed as a secondary mechanism in the deformation of the oxides. In coarse grained MgO, GBS resulted in extensive deformation in the vicinity of grain boundaries particularly at points of constrains such as triple points and boundary jogs where folds in the adjacent material were found as a result of the localized shear necessary for accommodation. This was intensified as corrugations in the boundaries developed so that continued sliding resulted in extensive shear in the region adjacent to the boundaries.[11] Relief from some of these high stress concentrations eventually resulted from grain boundary migration and polygonization.

As the grain size is reduced the contribution of GBS to total strain generally increases as a result of the increased boundary area. However, when the grain size approaches the width of the highly deformed region associated with GBS, it is expected that the contribution of GBS should become dominant and that a change in the microscopic deformation behavior may result.

Further support for such a change in behavior has been indicated in metals as a result of dislocation-boundary sliding interactions. It has been observed that the passage of a slip band through a boundary can cause some sliding of the boundary;[17] this is thought to occur as a result of incorporation of dislocations into the boundary and the movement of these dislocations along the boundaries. More recently sliding boundaries in bicrystals[39] and polycrystalline material[40] have been observed to emit dislocations into the grains; this dislocation emission has been explained to result from a sliding mechanism based on movement of dislocations in the boundary. It is then likely that as the grain size is reduced below the stable subgrain size, the boundaries become the principal sources and sinks of lattice dislocations and the sliding and accommodation processes become interdependent. This type of effect has been recently postulated to explain the superplastic behavior of fine grain metals.[41,42]

There is evidence for the existence of a somewhat similar condition in the various oxides at grain sizes below 5 to 10 μ at appropriate temperatures and strain rates. Deformation is marked by a high rate sensitivity, a strong grain size dependence and sometimes by strain hardening or a region

of transient creep which is much stronger than would be expected from diffusional creep. Microstructural evidence of GBS in terms of offset scratches displaced triple points or folded grains is frequent. Slip traces are also often seen in the cubic oxides; however, the contributions of dislocations is much more a matter of conjecture in Al_2O_3 and BeO.

This behavior has been studied most extensively in fine-grained Al_2O_3.[25] Material with a 1-2 μ grain size was very ductile in the range of 1300-1550°C; the flow stress was highly strain rate sensitive with values of 0.6-0.7 determined for the strain rate sensitivity index, m, defined by the relation:

$$\sigma = K \dot{\varepsilon}^{m} \tag{3}$$

where σ, and $\dot{\varepsilon}$ have been defined and K is a material constant. The strong grain size dependence was found to approximately fit the relation:

$$\dot{\varepsilon} \propto \frac{1}{G^{2.5}} \tag{4}$$

The measured strain rates were much greater than predicted by Eq. (1) using available self-diffusion data providing further indication this behavior was distinct from diffusional creep. As the grain size was increased up to 8 to 15 μ, m values increased up to about 0.8-0.9 which was taken to indicate a transition to control by diffusional creep at larger grain sizes.[25] A similar decrease in m from nearly 1 at 13 μ to 0.6 at 3 μ was seen in reviewing the data from earlier investigations of Al_2O_3 which had been interpreted in support of the diffusional creep mechanism.[30]

Limited tests of BeO of less than 10 μ grain size indicated similar non-Newtonian behavior.[43] This work also suggested that a transition from diffusional creep to GBS occurred with increasing stress. A change in m from about 1 to 0.5 with increased stress was reported for 2 μ Al_2O_3 suggesting a similar transition.[44] In both of these studies extended periods of strain hardening during transient creep were observed which provides further support for the fact that the process of GBS involves a fundamentally non-Newtonian process and is not simply a result of intergranular separation.

Microstructural examination of the 1-2 μ Al_2O_3 showed evidence of GBS such as displaced triple points. In addition, electron microscopy of thin foils indicated dislocations at some of the boundaries on which sliding had occurred.[25] It was concluded that the actual boundary sliding process was probably non-Newtonian involving grain boundary dislocations and boundary migration. The accommodation process was not positively identified; it was suggested to include diffusional creep and grain boundary migration. Some twinning was seen providing accommodation at points of high stress concentration such as triple points; however, it was not extensive enough to be a controlling mechanism. There was no positive evidence that dislocation glide had contributed to the necessary grain shape changes; however, the point is one of uncertainty since small grain sizes would allow lattice dislocations to be annihilated in the boundaries.

Rather similar behavior has been observed in MgO, UO_2 and ThO_2 although the greater ease of slip in these materials makes a clear differentiation among the various processes more difficult. A study of MgO at low strain rates in the temperature range 1100-1500°C indicated a change in behavior for grain sizes below 5 μ which was indicated by a decrease in m from 1 to 0.67 and a marked increase in activation energy.[18] The deformation at larger grain sizes was presumably controlled by diffusional creep rather than slip as a result of the low strain rate used.

Several studies of UO_2 with grain sizes below 10 μ have revealed similar behavior. For non-stoichiometric (oxygen-rich) material, deformation has been reported at temperatures down to 800°C with evidence of non-Newtonian behavior and extensive GBS.[15] In the range of 1000-1400°C a marked effect of stoichiometry was seen in which increased oxygen content resulted in much higher strain rates and a decline in m from 0.8 to 0.6 going from stoichiometric material to the limit of the phase field for oxygen enrichment.[35,46] Increased diffusivity with non-stoichiometry would result in higher strain rates; however, this does not per se explain the reduction of m. A similar change in stoichiometry reduces the resolved critical shear stress for slip on the $\{110\}$ $[1\bar{1}0]$ system* by a factor of three or four in this temperature range, and thus, apparently increases the ease of slip in polycrystalline materials.[23] This correlation further infers that the non-Newtonian GBS is related to the ease of slip behavior either in terms of material accommodation by slip or in terms of actual sliding by boundary dislocations.

In ThO_2 of 10 μ grain size at low strain rates a combination of GBS and diffusional creep was suggested. A reduction in m from 0.96 at 1430°C to 0.63 at 1790°C occurred along with microstructural evidence of GBS. This was interpreted as a transition in the controlling mechanism from accommodation by diffusional creep to limitation by GBS or slip at higher temperatures.[36]

In summary, values of m between 1/2 and 2/3 indicate that the deformation is limited by a non-Newtonian process. Although accommodation by slip within the grains might seem a reasonable explanation for this sliding of bicrystals of MgO has also been found to be non-Newtonian and to exhibit considerable strain hardening,[47] suggesting that the non-Newtonian process is intimately related to the sliding. The microstructural observation of GBS in 1-2 μ Al_2O_3 indicated that the dislocations were associated more with the boundaries than within the grains.[25] Observations of dislocations at the grain boundary after boundary sliding in a UO_2 bicrystal have also been reported.[22] These several observations all suggest the actual sliding is accomplished by movement of dislocations within the boundary and that the sliding itself is non-Newtonian. The Burger's vectors of the boundary dislocations and the orientation effects have not been identified so the exact mechanism cannot be further specified; similarly, information about the sources of grain boundary dislocations and the relation with the grain accommodation processes is necessary before this type of process can be completely accepted and understood.

The mechanism of fracture for materials deforming by GBS appears to be largely by intercrystalline separation resulting from the growth of cracks

* This is the more difficult to activate slip system in UO_2 and is necessary in addition to the $\{100\}$ $[1\bar{1}0]$ system to satisfy the Mises requirement.

and voids at the boundaries. The electron microscopy of Al_2O_3 showed the development of small voids at triple points as a result of GBS.[25] Cavitation on the boundaries normal to the tensile axis has been seen in MgO,[18] ThO_2,[22,36] and UO_2.[35,45] Investigation of UO_2 indicated that intergranular cracking was more severe for the stoichiometric material;[46] it was suggested that more rapid grain boundary migration in the oxygen-rich material may have been responsible for the reduced boundary cracking;[46] it seems likely that the low yield stresses for slip which result from non-stoichiometry[23] may also contribute to reduced cracking. It can be expected that any factors which ease the problem of accommodation or allow easier boundary migration will result in increased ductility by reducing stress concentrations and preventing the growth of crack nuclei. The presence of porosity and impurities at the boundaries can be expected to reduce ductility by restricting boundary migration and weakening the boundaries.

Although a quantitative study for the oxides at high temperature does not exist, several investigators have suggested that greater ductility and higher fracture strengths result at finer grain sizes. This seems intuitively appealing for several reasons. A finer grain size reduces the amount of sliding per boundary at a given strain as a result of the increase in boundary area. If cavitation results directly from sliding, as has been shown for Cu,[48] then the reduced sliding per boundary should result in less severe cavitation at a given strain. Changes in mechanism which modify the contribution of GBS will, of course, modify this somewhat.

Finer grain sizes should also reduce stress concentrations and thus reduce the tendency for cracking. If the shear stress on a boundary is relaxed by sliding, then a large stress concentration will develop at the points of constraint where sliding is restricted such as triple points or ledges. This stress concentration will be proportional to $\sqrt{c}$ where 2c is the length of relaxed boundary.[49] This length will be approximately the grain boundary facet size, unless constraint at ledges reduces it. As a result, finer grained materials should develop less severe stress concentrations at obstacles thus reducing the tendency for crack formation. Although these factors are both significant, additional factors resulting from differences in GBS mechanisms may prove to be equally important.

For a system in which there is sufficient accommodation and boundary migration to inhibit cavitation during GBS, large elongations should be obtainable. The high strain rate sensitivity which exists will provide excellent neck stability[50] eliminating the need for strain hardening for this purpose. The actual amount of strain hardening expected with this mechanism is unknown as are the possible effects upon fracture stress. However, it seems likely that the most critical problem is the elimination of grain boundation cavitation and cracking both for good ductility and to prevent degradation of subsequent properties.

C. Areas for Investigation

Several areas are indicated as fruitful for further investigation and forging studies. The above review suggests two alternative approaches as

most promising for initial investigation. One, is to take advantage of the known ductility available from GBS in very fine materials; Al_2O_3 is the most appropriate material for investigation in this area. The second alternative is to forge under conditions where full ductility from slip can be obtained; for this MgO appears to be the most appropriate material. Alternatives for both of these processes utilizing other compositions in the Al_2O_3-MgO system are also worthy of investigation.

The Al_2O_3 + 1/4% MgO system is being utilized initially for study in this area. High quality materials of about 1 μ grain size can be prepared and the system is exceptionally stable with respect to grain growth. For MgO of high density and purity, grain growth is sufficiently rapid that grain sizes below about 5-10 μ are not stable at 1400°C even for relatively short times.[51] In addition to offering good promise of success, the utilization of fine grained starting materials and forging at moderate temperatures provides a method for retention of a fine grain size in the finished piece; this is highly desirable for many of the subsequent properties of interest. Although there has been considerable work to date utilizing porous starting materials[2,4] this approach is not being considered here; only fully dense preforms are being used.

The work to date has indicated that fully ductile behavior by slip in MgO does not occur until about 1800°C and that for hot pressed materials it may be as high as 2200°C. These results were born out by the extrusion work by Rice in which greater problems resulted with hot pressed bodies than with single crystals or fused material.[1] This indicates that every effort must be made to obtain high purity, high density materials and that investigation should be primarily concentrated at temperatures in excess of 2000°C.

The eventual forging investigation of $MgAl_2O_4$ is felt to be warranted for several reasons. This sytem apparently has sufficient slip systems to provide adequate ductility for forging, and in fact, is the only oxide in which the primary system provides five independent systems.[21] Investigation of it should provide insight into additional problems which may be posed by a mixed oxide compound.

The desire for a fine grained system which is stable at high temperatures may be provided by two phase compositions in the Al_2O_3-MgO systems. Creep studies with a series of compositions between MgO and $MgAl_2O_4$ indicated considerably higher strain rates under comparable conditions for intermediate compositions resulting in two-phase microstructures.[52] This was probably at least in part the result of the finer grain size obtained in the two-phase materials under similar conditions. This system should also provide interesting mechanistic insight since both phases are relatively ductile. Fine-grained, two phase compositions of Al_2O_3 and $MgAl_2O_4$ would also be expected to provide a stable, fine grained structure and investigation should provide insight into mechanisms involved in GBS.

As previously mentioned, a combination of mechanical testing and forging will be done as well as microstructural evaluation. Areas under investigation include the dependence of flow stress on temperatures, strain, strain rate and microstructure and similarly the dependence of fracture upon

these same variables so that the areas of maximum ductility can be identified. Accurate data which can be used to develop constituitive equations and mechanistic understanding are desired. Testing will be done in several modes including flexure, tension and torsion in order to assess the effect of deformation mode upon ductility and to provide flexibility in testing. Where feasible, testing will be to failure to provide information on both flow and fracture. Investigation over wide ranges of strain rate is planned in the temperature range of 1300-1900°C for Al_2O_3 and $MgAl_2O_4$ and 1400-2200°C with emphasis at the high end for MgO. Multiple loading, with and without intermittent annealing will be utilized to provide information on recrystallization and recovery behavior which may affect formability.

The conditions for forging experiments will be dictated by the results of the mechanical property tests in order to optimize formability. Shape forging will be used extensively, with deep drawing of a hemisphere to be studied initially. Shape forging is desirable for study in comparison with upset forging or extrusion because it generally involves some tensile deformation. While this is a more severe condition it provides a broader base of understanding for subsequent deformation processing of ceramics. The ability to produce final shapes is also a desirable goal in itself. Analysis of the plastic flow during forging and failure analysis will be utilized in order to allow interpretation of the results and correlation with the mechanical property data which will be obtained. These results will be utilized to provide modifications in forging conditions and tooling design. A few upset forgings are planned to provide material for evaluation of the effects of forging upon subsequent properties.

III. RESULTS

The primary effect of the program has been concentrated on mechanical tests of fine-grained Al_2O_3. A few forgings were done which provided valuable information about techniques and problem areas. The microstructural evaluation of the test results and the forgings are treated together here for greater clarity.

A. Mechanical Tests

Considerable testing of Al_2O_3 was done in order to investigate both flow and fracture behavior. All of the testing was done in four-point flexure in the temperature range 1250-1750°C. Three particular series of tests were done. One was a series in which multiple bending of bars was done to assess the effects of high strains. A second group was done to clarify the effect of grain size on the flow stress and to indicate whether a change in mechanism could be determined by a change in the grain size dependence. Finally, a number of tests at constant temperature were performed to determine the effect of strain rate on the fracture stress at high temperature.

Most of the materials tested were hot pressed to densities of 99.7% or greater. These all had an addition of 0.1% or 0.25% MgO to retard grain growth; the initial grain sizes were primarily in the ranges of 1-2 μ. In addition, some sintered Lucalox specimens with a grain size of 15 μ and a density of 99.2% were tested.*

The testing was done in two different argon atmosphere furnaces, both of which utilized four-point bending fixtures with the inner knife edges at the quarter points. Both are constant cross-head speed devices with provisions for changing the speed during a test. Square knife edge inserts with a small radius on the edge were used for load supports. Most of the multiple bend tests were done with specimens which were 0.050 x 0.100 inch with a 0.750 inch loading span and were tested in a molybdenum wound furnace. A few multiple bend tests and all of the others were done on 0.100 x 0.200 inch specimens in a fixture with a 1.500 inch outer knife edge length which was heated in a Centorr tungsten mesh furnace. Deflections were measured directly with a set of probes which actuated an LVDT; deflection and load were recorded continuously versus time.

1. Multiple Bend Tests

Multiple bend tests were run in order to assess the effects of larger total strains as well as to indicate any effects of interrupting or reversing the strain or of annealing. The test schedule called for bending the specimen to the desired outer fiber strain, usually 5%, (the limit of the apparatus); the specimen was then reversed and bent back through the range $-\epsilon_o$ to $+\epsilon_o$ in each cycle. For some specimens the tests were interrupted and the specimens held at temperature for various amounts of time to assess

*All grain sizes were measured by the linear intercept method and are reported as $G = 3/2\ \bar{L}$..

any effects. The process of bending could be continued through several cycles or until failure occurred. For a given specimen all of the testing was generally at the same strain rate.

These tests were done only on fine-grained specimens at lower temperatures to reduce grain growth. Most of the tests were done on a group of small specimens designated FLUX, which were hot pressed with 1/4% MgO and had initial grain sizes in the range 1.7-2.0 μ; these were done over a range of strain rates at 1450°C. A few additional tests were also done on some large samples of similar materials. The samples were all visually examined between cycles for evidence of cracking; and for a few the surfaces were replicated in order to allow examination with the electron microscope after each cycle.

The load-deflection curves indicated several interesting features, particularly the FLUX materials. However, the problem of reducing these to stress-strain curves proved to be more formidable than had been initially anticipated. A typical curve is shown in Figure 1; the apparent stress was calculated from the elastic formula (see equations A3 and A10) and so is directly proportional to the measured load. All of the curves showed similar features of a significantly reduced load upon reversal and a build-up of load during each cycle. The FLUX materials all exhibited a trend of increased load for each successive cycle; this feature was much less pronounced for the other materials, but the curves were otherwise similar. The shapes of these curves are suggestive of rather interesting physical behavior; in addition to the general trends noted, the curves occasionally showed a drop in load after the initial build-up, reminiscent of materials which exhibit a yield drop. The irregular behavior seen in Figure 1 was also seen in most of the curves.

Before conclusions could be made about physical behavior suggested by these curves, an investigation of possible effects resulting from curvature, large deflections and friction on the bend tests was required. The results are presented in the Appendix. The results indicate that the general shape of the curves, i.e., an increasing load during the test and a lower load on reversal, can be explained in part by the development at large curvature of horizontal load components at the supports, and also by a shift in the point of contact with the supports. The horizontal loads are significantly affected by friction, however, so a quantitative correction cannot be made without an assumption about the coefficient of friction at the supports. Further uncertainty results from the fact that the specimens became somewhat irregular after several cycles so the strain was not uniform in them.

Examination of the deflection curves indicated that many of the fluctuations in the load correlated with changes in the strain rate. Although the machine speed is not as constant as desirable, especially at the lowest speeds, the strain rate fluctuations were usually in excess of the cross-head speed variations. These are thought to be caused in part by some hardening in the gage section resulting in increased deformation in the moment arms and also by variation in the friction which alters the relative moments in the gage section and movement arms.

As a result of these several uncertainties, it was decided that attempting to reduce the entire load-deflection curves to true stress-strain curves was not warranted; they were calculated as apparent stresses using

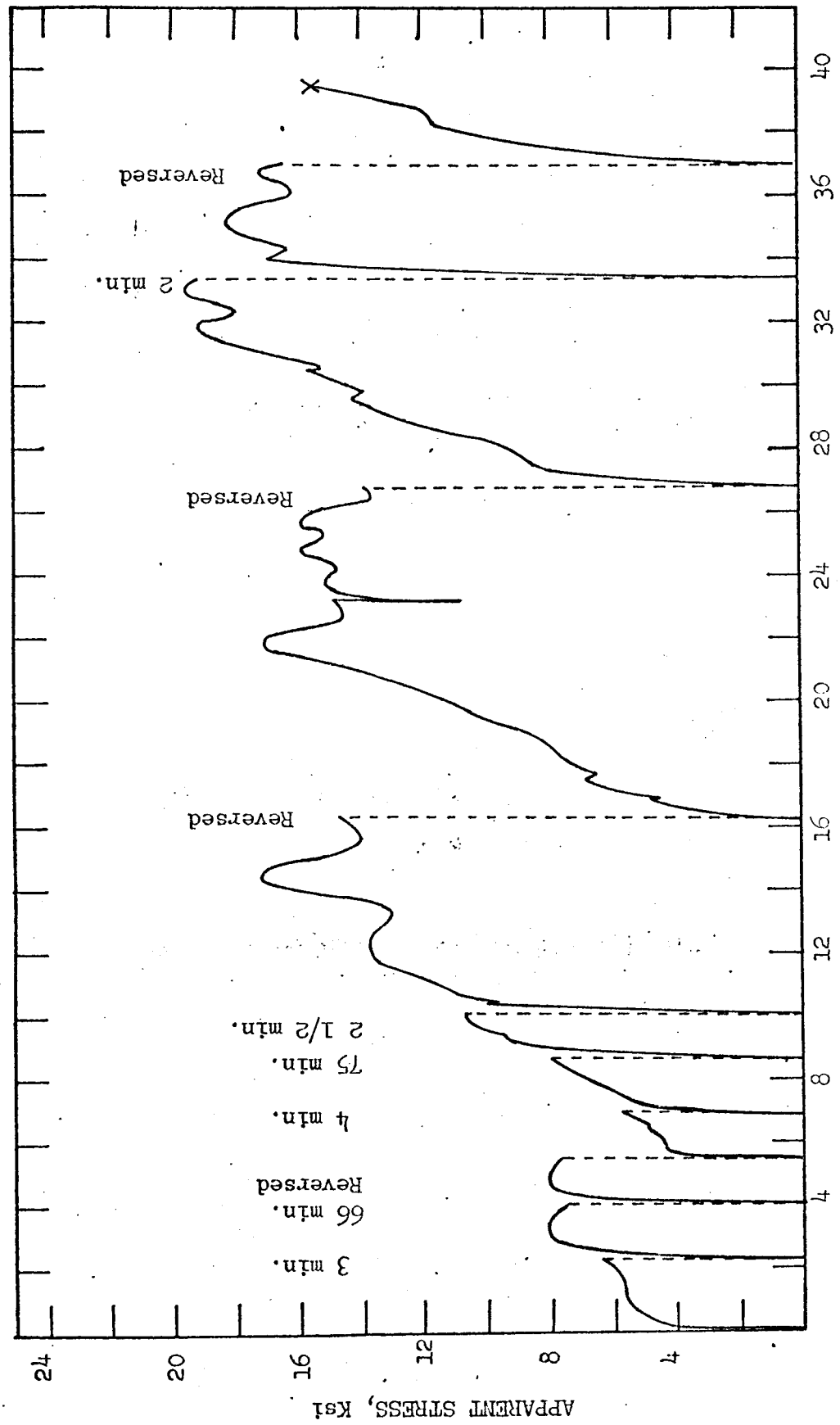

Figure 1. Apparent Stress vs. Strain Curve for Specimen FLUX-30 Tested at 1450°C.

the elastic formula for comparative purposes. Although the general shape of the curves can be qualitatively predicted by the effects of horizontal loads and a shift in the point of contact at the load supports, some of the other features are still unresolved. For instance, the shape of the earlier parts of the curves could be substantially altered by changes in the coefficient of friction; as a result, it is impossible to distinguish whether the material simply has an asymptotic approach to a steady-state stress as would be expected for a visco-elastic material, or whether some type of yielding behavior occurs. Similarly, this uncertainty prevents a judgement about whether the flow stress is identical upon reversal of the direction of strain, or whether there is an actual reduction of the flow stress upon reversal (i.e., Bauschinger effect). By postulating appropriate variations in the friction during a test or from test to test, possible explanations for several effects can be obtained; this does not, however, constitute a proof that the effects are entirely test artifacts, but it does prevent firm conclusions about alternative physical explanations.

From the fluctuations in loads with variations in strain rate, it could be seen that the strain rate sensitivity remains high even at the highest total strains investigated. A quantitative assessment of the strain rate sensitivity, m, with strain was not attempted, however. For tests where the specimens were unloaded and reloaded, small differences in the new strain rate seemed to have a greater effect on the new load than the time of holding at temperature. This prevented a firm assessment of the magnitude of recovery during unloading, but indicated no significant recovery seemed likely to be occurring in times up to an hour.

The analysis previously referred to (see Appendix) indicated that the error in the simply calculated stress, should be quite small at the midpoint of the test when the bar is nearly flat. In order to show the effect of the increased strain in successive cycles, the apparent stress taken at the midpoint for each cycle was plotted against the total strain. These are plotted in Figure 2 for several specimens. Several features indicated that the behavior is not simple strain hardening. The shape of the curves indicates that the hardening from cycle to cycle does not fit a normal parabolic hardening curve as is frequently found for metals; the data would better fit a nearly linear hardening curve. It can also be seen that the data for Specimen FLU5-6, taken from a set of specimens previously tested,[25] showed very little increase in stress through several cycles; this was a large specimen and was tested at 1415°C, but otherwise the procedure was similar. Very slight hardening was also seen for a couple of other specimens at 1415°C. For the specimens which exhibited the greatest hardening, the bending became less uniform after several cycles; as the gage section became harder relatively more strain occurred in the moment arm regions. This effect was less pronounced in those specimens exhibiting limited hardening.

For two of the FLUX specimens, replicas were taken of at least one surface after every cycle, for examination in the electron microscope. From these, grain growth was observed during the course of the tests. For comparison, a control sample was included in several of the test cycles and similarly replicated and examined. The grain size measured after each cycle is plotted in Figure 3a. These data suggest that some normal grain growth occurred for these materials, but that additional growth occurred as a result of the concurrent straining. The strain rate of FLUX-32 was higher than for FLUX-33 so the time per cycle was actually somewhat shorter. Some

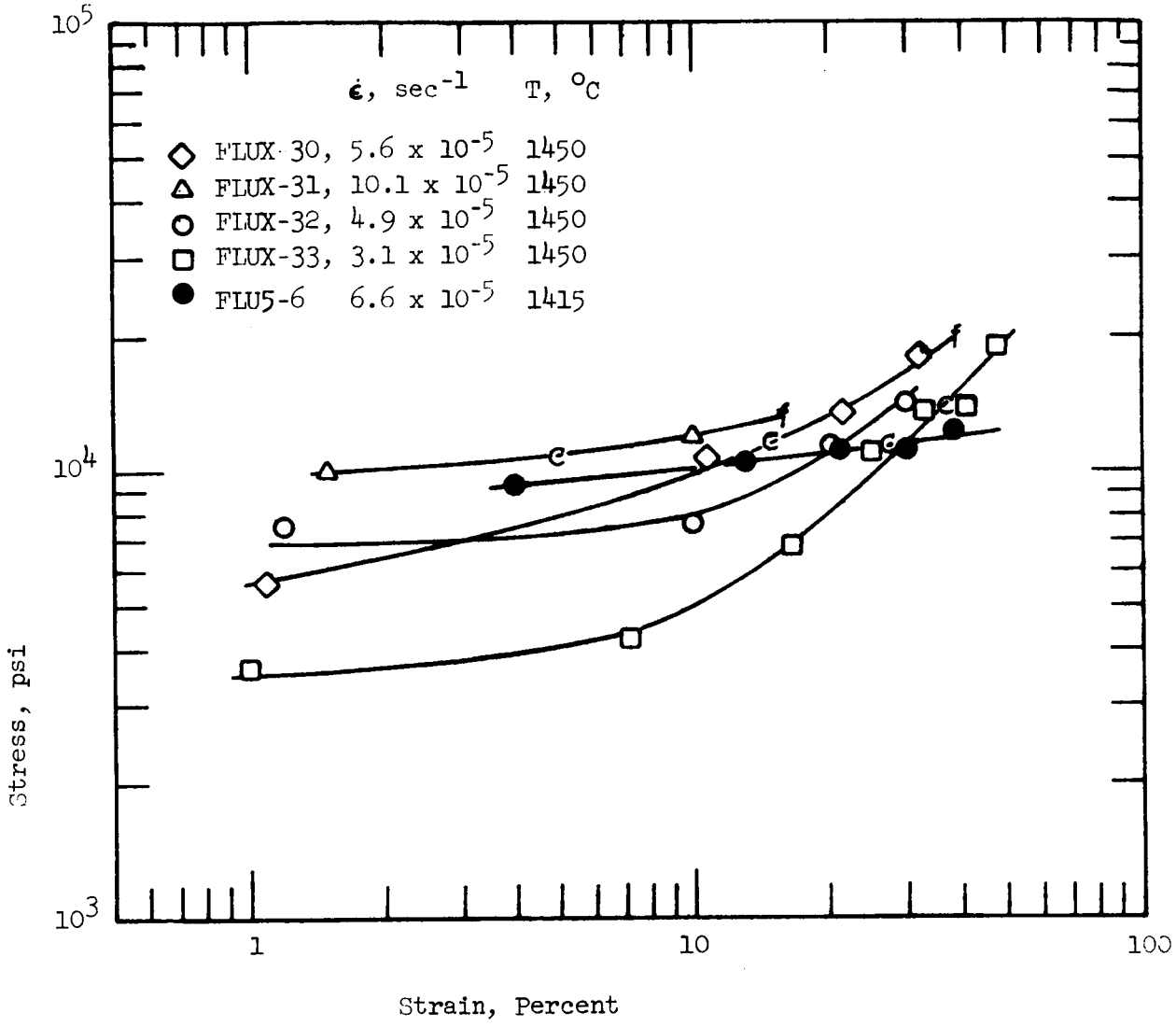

Figure 2. Apparent Stress versus Strain Relations for Multiple Bend Tests. The data were taken from the midpoint of each cycle. The letter 'C' is shown on the curves at the strain at which cracks were first seen; the letter 'f' is also included at the strain at which fracture finally occurred.

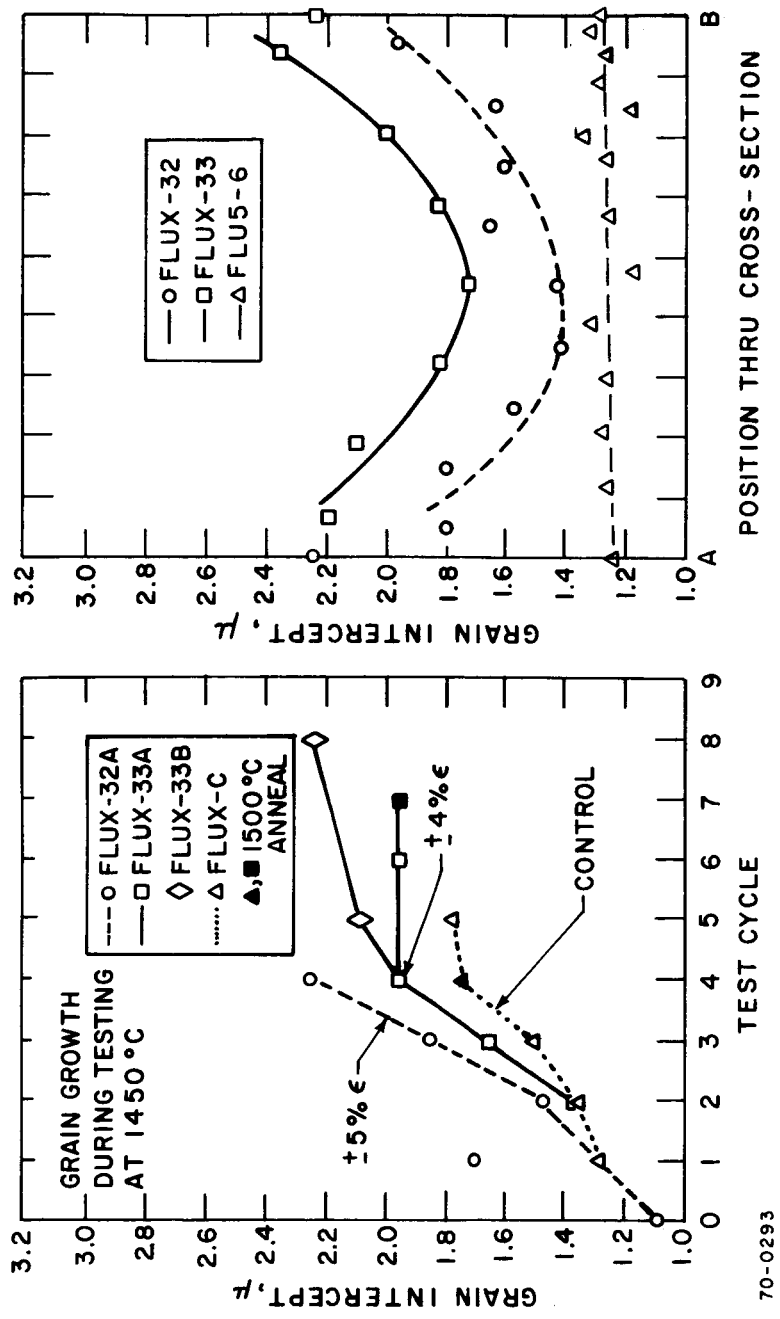

Figure 3 EVIDENCE OF STRAIN ENHANCED GRAIN GROWTH. PART (a) SHOWS THE SURFACE GRAIN SIZE MEASURED AFTER SUCCESSIVE TESTS IN TWO MULTIPLE BEND SPECIMENS AND FOR A THERMAL CONTROL SAMPLE. PART (b) SHOWS A PLOT OF GRAIN SIZE THROUGH THE CROSS-SECTION FROM SURFACE A TO SURFACE B FOR THESE TWO SPECIMENS PLUS AN ADDITIONAL ONE, FLU5-6, WHICH WAS TESTED AT 1415°C. (NOTE THAT THE UNCORRECTED GRAIN INTERCEPT IS PLOTTED IN THIS FIGURE.)

of the scatter and missing points are accounted for by the fact that the grain size was extremely difficult to measure on some of the compression surfaces (e.g., FLUX-32, #1).

These data have some uncertainty associated with the possibilities of loss of dopant (MgO) from the surface, surface contamination from the furnace, and the effect of surface grain boundary interactions resulting in higher grain boundary mobility. To provide alternative evaluation, the two specimens were cross-sectioned, polished, etched and replicated. Photographs were taken at regular intervals through the cross-section. The grain size, measured from these, is plotted as a function of position through the cross-section in Figure 3b. These results indicate an increase in grain size from the center out to each surface with maximum grain sizes at the surface of about 3.0 μ and 3.7 μ for FLUX-32 and FLUX-33, respectively, compared with a starting grain size of about 1.8 μ. This is as expected for strain enhanced grain growth since the strain is approximately zero at the center and increases linearly to the surfaces. (Actually, the neutral axis tends to move toward the concave surface so that in multiple bending it moves back and forth past the center and there is no region of zero strain.) A similar grain size scan was done for Specimen FLU5-6 and the results are included in Figure 6b; it is seen that there is almost no grain size variation in the specimen and that the final grain size of 1.9 μ is only slightly larger than the initial value of 1.8 μ for this billet.

Comparison with Figure 2 shows that considerable hardening occurred for the specimens which exhibited strain enhanced grain growth, but that very little hardening occurred for the specimen in which almost no grain growth occurred; nominal grain size measurements indicated some growth also occurred in FLUX-30 and FLUX-31. This result is not surprising since previous work at low strains showed that at a constant strain rate the stress increases approximately with the square of the grain size. Utilizing this dependence, most of the observed hardening can be accounted for by the increase in grain size during the course of the tests. Because of the uncertaintites in the stress calculations, it cannot be determined whether there is an additional component of hardening; the low rate of hardening for FLU5-6 suggests, however, that the grain growth effect is the major contribution.

Strain enhanced grain growth is not particularly surprising because the stress concentrations and boundary jogs which typically result from GBS must provide a strong driving force for boundary migration. The surprising feature is that it did not occur in all of the specimens. The FLUX and FLU5 material were thought to be identical so that there is no known material difference to explain the difference. It is possible that the slightly lower temperature used for FLU5 is responsible for the reduced migration; it seems surprising, however, that the effect of a 35°C difference would be so large. Although it is not clear why growth occurs, it seems apparent that when it does occur it may be enhanced by concurrent straining and that it causes a substantial hardening of the material.

The specimens were examined for detection of cracks after each cycle. Cracks were seen to develop in specimens and grow to surprisingly large sizes before causing fracture. An example of the growth of such a crack can be seen in Figure 4 which shows the development of a rather large

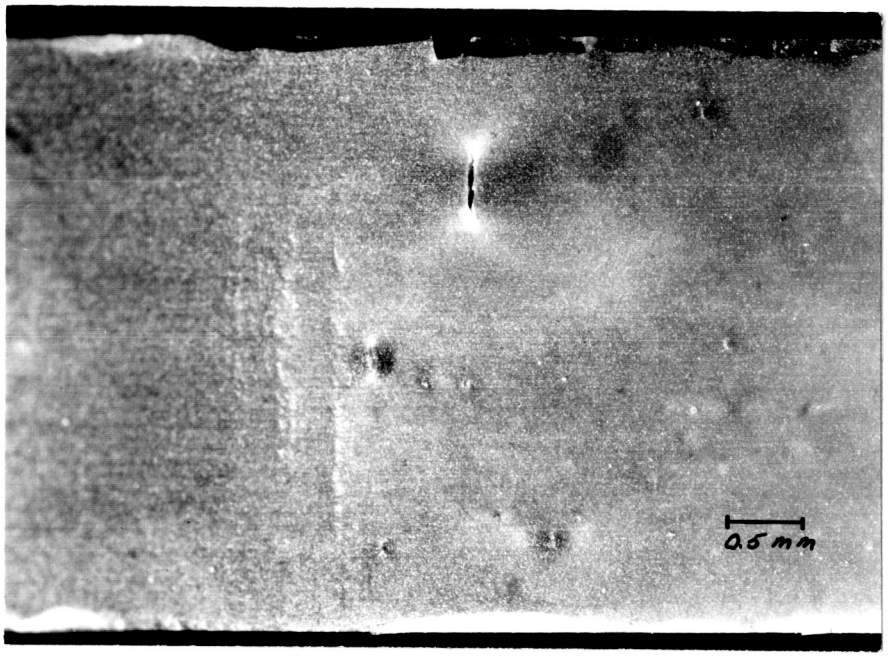

#5116 (a) 20X

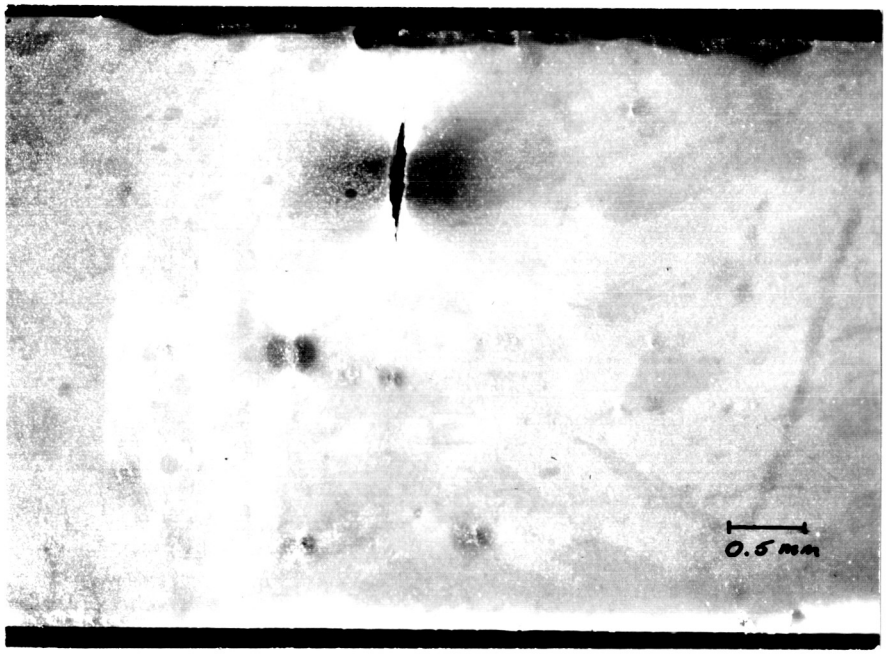

#5116-1 (b) 20X

Figure 4. Crack Seen in Surface of Specimen FLUX-30 During Multiple Bending, (a) After Bend No. 2, (b) After Bend No. 4.

crack and the formation of several smaller ones. Eventually cracks such as these grow sufficiently large that a rapid, apparently brittle propagation occurs causing fracture of the specimen. Examination of the specimens indicated the cracks tended to form in areas which could be initially identified as discolored spots in the specimens. These are thought to contain residual pore nests at their center although some of them may contain impurities also.

On the curves in Figure 3, the letter C is used to indicate the strain after which cracks were first seen in the various specimens. In addition, the letter F is used to indicate the strain at which fracture occurred. Because of the limited number of points and the uncertainty about the stress values, caution should be used in evaluating these results. At the very least, it appears certain that at lower strain rates and stresses, more strain is possible before visible cracks develop. Further, it seemed qualitatively as though the rate of growth was more rapid at higher rates. Some of the scatter of these data were also explained by variations in the severity of such defects in the specimens. It could be inferred from these data that cracking did not appear until after the stress built up to a value in excess of 10,000 psi; such a conclusion is not warranted by the limited data at hand.

2. Strain Rate - Grain Size Dependence

As previously discussed, there is considerable evidence to indicate that as the grain size is decreased in Al_2O_3, there is a shift in the controlling mechanism from diffusional creep to GBS. In previous work[25] the strain rate was found to be proportional to $G^{-2.5}$; this non-integral value may be representative of a transition between two mechanisms. In order to clarify this point a series of change-of-rate tests were done for two materials to confirm and extend the previous data. The tests were done by straining the specimens at a constant rate until a constant flow stress was obtained and then increasing the rate in increments and holding until a new constant flow stress was achieved.

Two different starting materials were each tested at three temperatures. After the tests most of the specimens were fractured and the fracture surface replicated for grain size measurement in the electron microscope. A hot pressed billet, C126C, of Al_2O_3 + 1/4% MgO was used which had an average grain size after testing of 1.2 μ; this is finer than any of the materials previously investigated and was tested between 1251°C and 1415°C. To confirm previous work a batch of specimens of sintered Al_2O_3 + 1/4% MgO were obtained and tested in the range 1564°C to 1750°C; these had an average grain size of 15 μ. The load-deflection curves were reduced using equation A1 as described in the Appendix, for these conditions strain hardening was taken to be negligible.

The results are presented in logarithmic plots of stress versus strain rate in Figures 5 and 6. The data generally agreed with the previous results[25] in that the finer grained materials had lower values of m than the coarse grained ones. For the fine grained material, m was between 0.65 and 0.71 which was slightly higher than the 0.61 to 0.66 found in the previous work for 1.8 μ material. For the 15 μ sintered specimens, m was about 0.9 in contrast to values of 0.8 previously measured. These may reflect differences

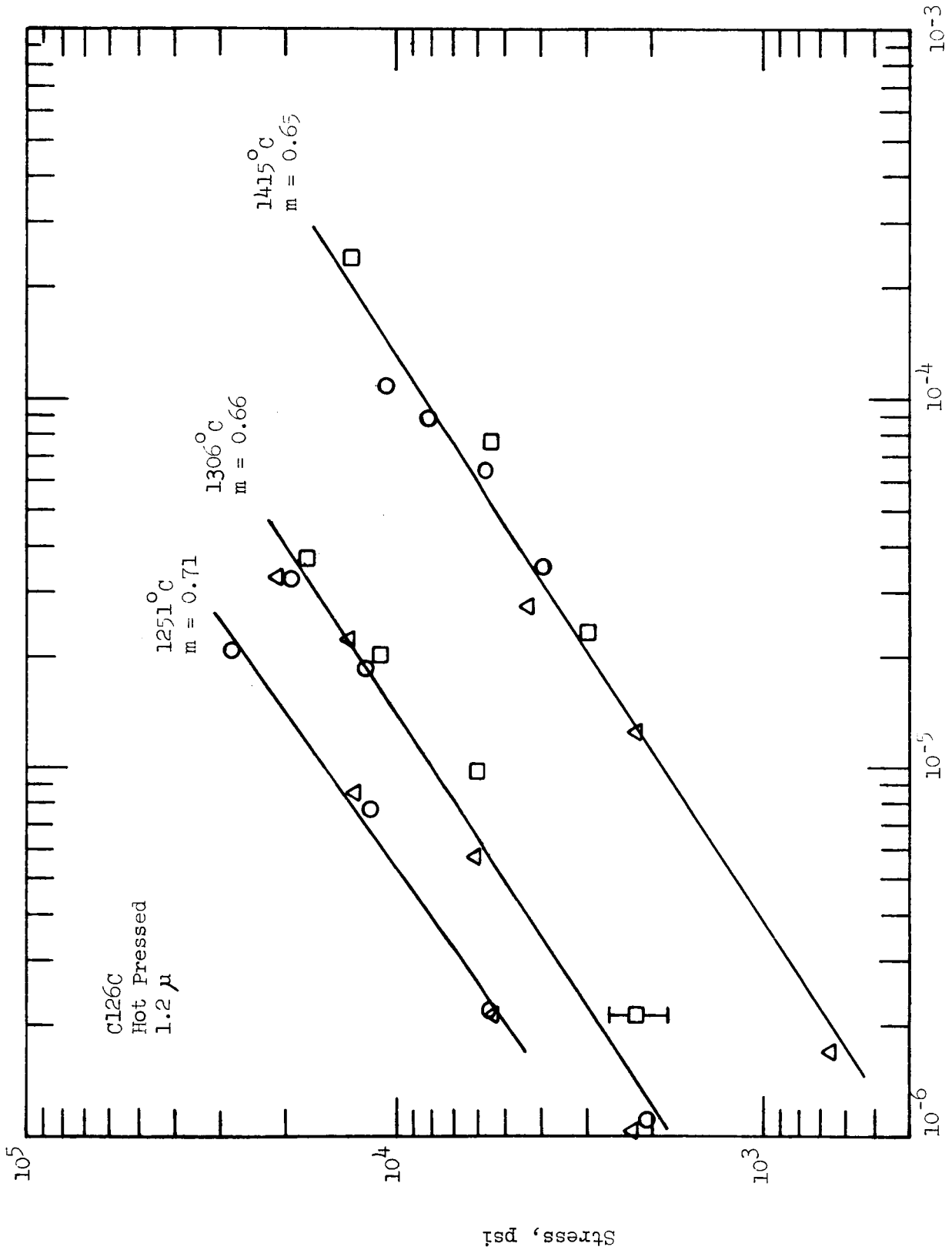

Figure 5. Stress-Strain Rate Curves for the Fine-Grained, Hot Pressed Material, C126C.

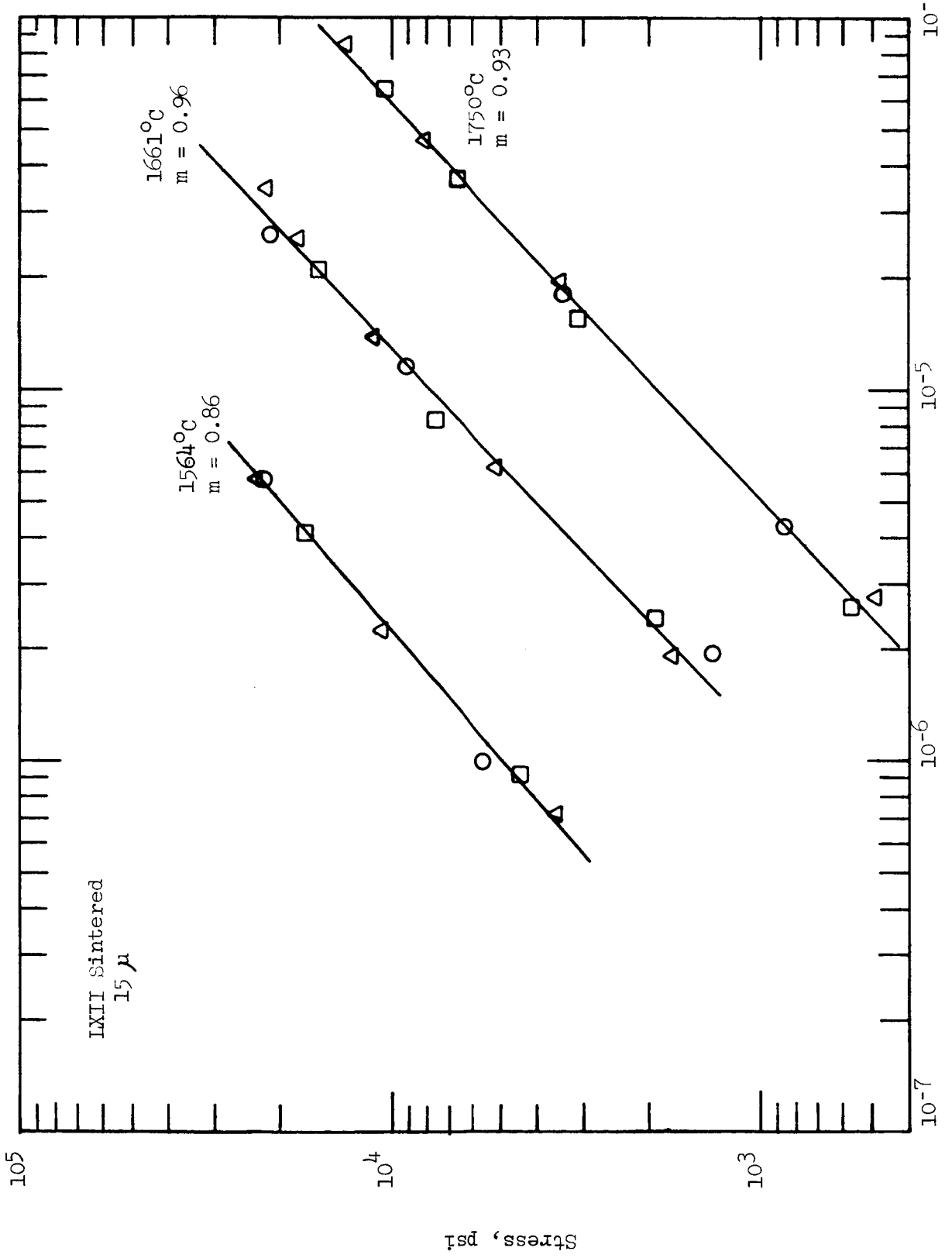

Figure 6. Stress-Strain Rate Curves for the Sintered Material, LXII.

in frictional or other effects since the previous work was done in a different fixture in an air furnace.

Activation energies were determined for these materials by plotting the strain rate at 5000 psi versus 1/T. These are plotted on a curve, Figure 7, which includes earlier work for comparison. It can be seen that the sintered material has essentially the same activation energy, but that it had a much lower strain rate than the 14 μ material previously tested. The fine grained material had a lower activation energy than for slightly coarser materials in keeping with the general trend, but it was not found to have a higher strain rate as would have been expected.

For the fine grained material the specimens tested at 1415°C had a grain size about 10% higher than those tested at 1251°C. This is probably indicative of some grain growth at the higher temperatures; this would contribute somewhat to the low value of activation energy. Normalizing for this affect, assuming a grain size dependence of $\dot{\epsilon} \propto G^{-2.5}$, would raise ΔH to 107 Kcal/mol from 99 Kcal/mol.

A further indication of this dependence of activation energy on grain size can be seen in Figure 8 in which the activation energies determined for deformation are plotted against the grain size. For comparison, the data from several other investigators[29,30,44,53] has been included. It can be seen that the trend continues to large grain sizes where a value of 185 Kcal/mol was found for 100 μ material in contrast with a value of about 100 Kcal/mol for 1 μ material. The data at coarser grain sizes were taken at higher temperatures so that a dependence on temperature would be reflected as a grain size dependence. Examination of Figure 7 indicates that the activation energy was independent of temperature for each material; further, there is sufficient overlap of various of the data that it is thought that the trend reflected is primarily a reflection of a grain size dependence, not a temperature dependence of activation energy. The specimens marked CR in Figure 7 had a duplex microstructure and were thought to be atypical so poor agreement with these specimens is discounted somewhat. The only other point which does not fit adequately is that at 3 μ; there is no known explanation for this.

The difference in strain rate for the two materials tested here can be seen better in Figure 9 where the grain size-strain rate dependence is plotted for the present data in comparison with previous results.[25] This plot was obtained by taking the strain rate for each material from the curves in Figure 7 at a temperature of 1528°C. It can be seen that the present data are at a factor three to five lower strain rate than would be predicted from the previous results. The cause of this is not known. The test procedures for the two sets of tests were essentially similar as were the analytical techniques and assumptions, except for the fact that the previous tests were performed in a different furnace in an air atmosphere in contrast with the present tests which were done in commercial grade argon. It is perhaps possible that the defect concentration in Al_2O_3 could be reduced in the lower oxygen pressure and cause a reduction in the diffusivity sufficient to cause such a reduction in strain rate, this cannot be accepted as the cause without greater assurance that the samples are not otherwise different.

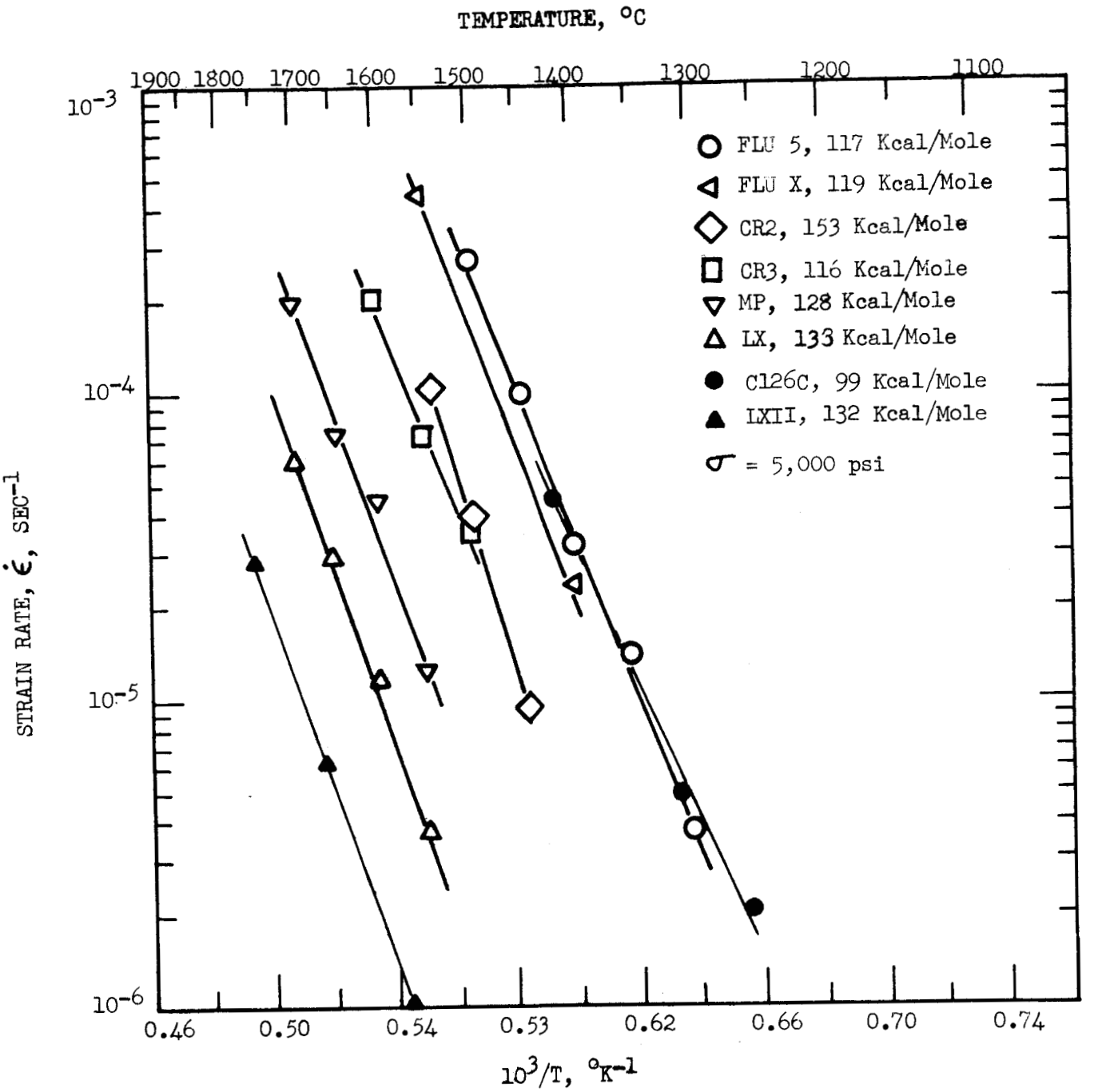

Figure 7. Strain Rate versus 1/T Showing the Activation Energy for Deformation. The present results are denoted by filled symbols and are shown in comparison with previous work.[25]

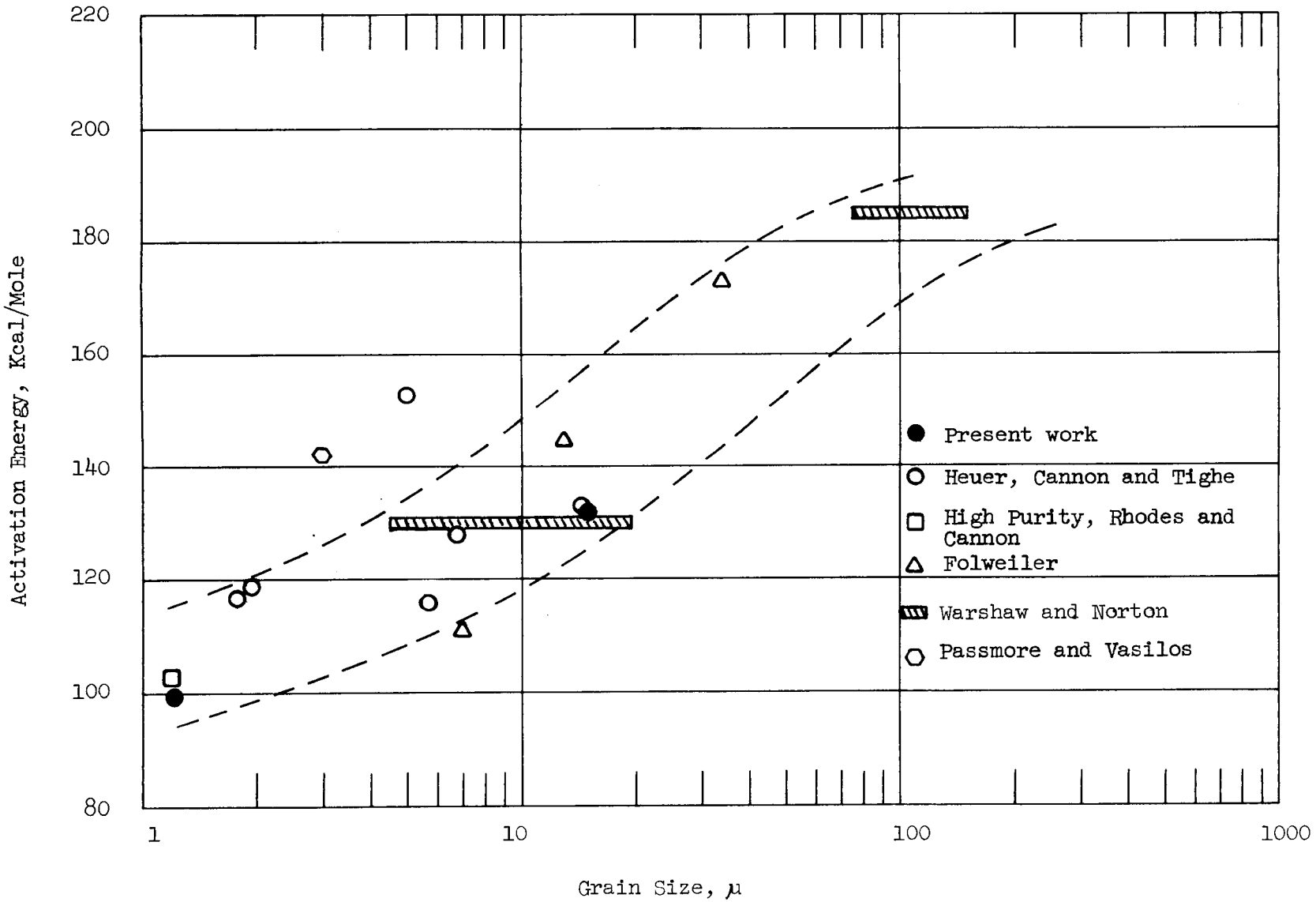

Figure 8. Dependence of the Activation Energy for Deformation on Grain Size. The grain sizes for the various investigators have been normalized to the same correction factor. The values from Folweilers data were determined by the present authors. The values at 99 and 111 Kcal/Mole may be somewhat low as a result of grain growth.

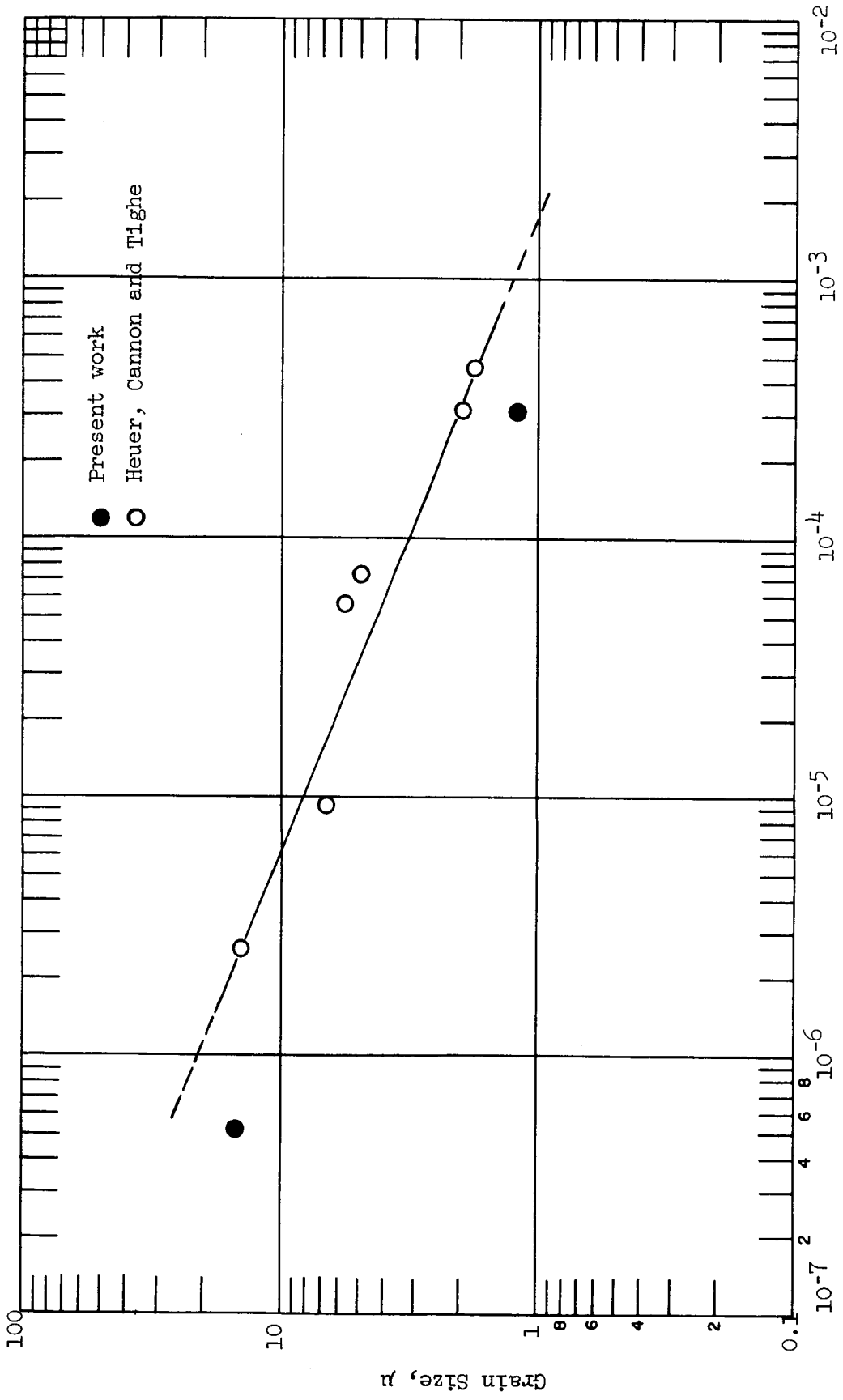

Figure 9. Plot of the Strain Rate Dependence on Grain Size for Various Materials at 5000 psi Stress and 1528°C. The line is that of the previous work[25] with the present results denoted by filled symbols.

The sintered materials are nominally the same, although they are from different batches and may contain an unknown difference such as an impurity phase at the boundaries; this should be investigated by comparing specimens from the two different batches. The two hot pressed materials were both made from similar grades of Al_2O_3 powder and using similar techniques. The previous material, Billet FLU5, had a dark color in comparison with C126C which was light grey. This difference is thought to be caused by a difference in the carbon content resulting from slight differences in the preparation techniques. The dark color of the FLU5 may indicate a carbon content in the range of 0.05-0.1%, whereas that for the grey material would be somewhat less than this.* A quantitative comparison of the two materials must be done before this effect can be evaluated with confidence.

The present results do not provide clarification of the grain size dependence which was anticipated. Nevertheless, the results are suggestive of either a compositional effect or an atmosphere effect on deformation rate. These warrant further analysis since either explanation has considerable importance on the identification of the deformation mechanisms and also practical affects on forging. The possibility of an effect from carbon is quite interesting since it would be expected that this would have a considerable influence on the tendency for cavitation during deformation because of the development of an internal gas pressure.

3. Fracture Stress-Strain Rate Dependence

The multiple bend tests have indicated that rather large cracks can grow in a stable mode during deformation of a sample. Eventually these become sufficiently large that they propagate rapidly leading to failure of the specimen. In order to provide further information with which to evaluate the formation and propagation of these cracks, tests to determine the effect of strain rate on fracture stress have been conducted at 1415°C.

A series of constant strain rate tests were run over a range of strain rates which was sufficiently broad that essentially brittle fracture resulted at the high end and fully plastic behavior occurred at the low end. The specimens were all from a billet, C79 of Al_2O_3 + 0.1% MgO hot pressed to over 99.7% density which had an average grain size of 2.5 μ. The load deflection curves are being analyzed using equation (A1) so that the true stress at fracture can be determined and the effects evaluated both with respect to the effect of strain rate per se and the effect of strain on fracture.

Since these analyses are not yet complete, the approximate fracture stresses determined from the elastic formula are presented in Figure 10. The points marked fracture stress are for specimens which failed with little if any plastic strain since the steady-state flow stress would have been in excess of the fracture stress. The points marked yield stress are for specimens for which the flow stress is less than the fracture stress and failure had not occurred before the test was terminated at an outer fiber strain in excess of 4%. The two at lower strain rates were rebent several times at the same strain rate and no significant hardening developed. Small cracks

* Private communication, John E. Niesse, Avco Corp.

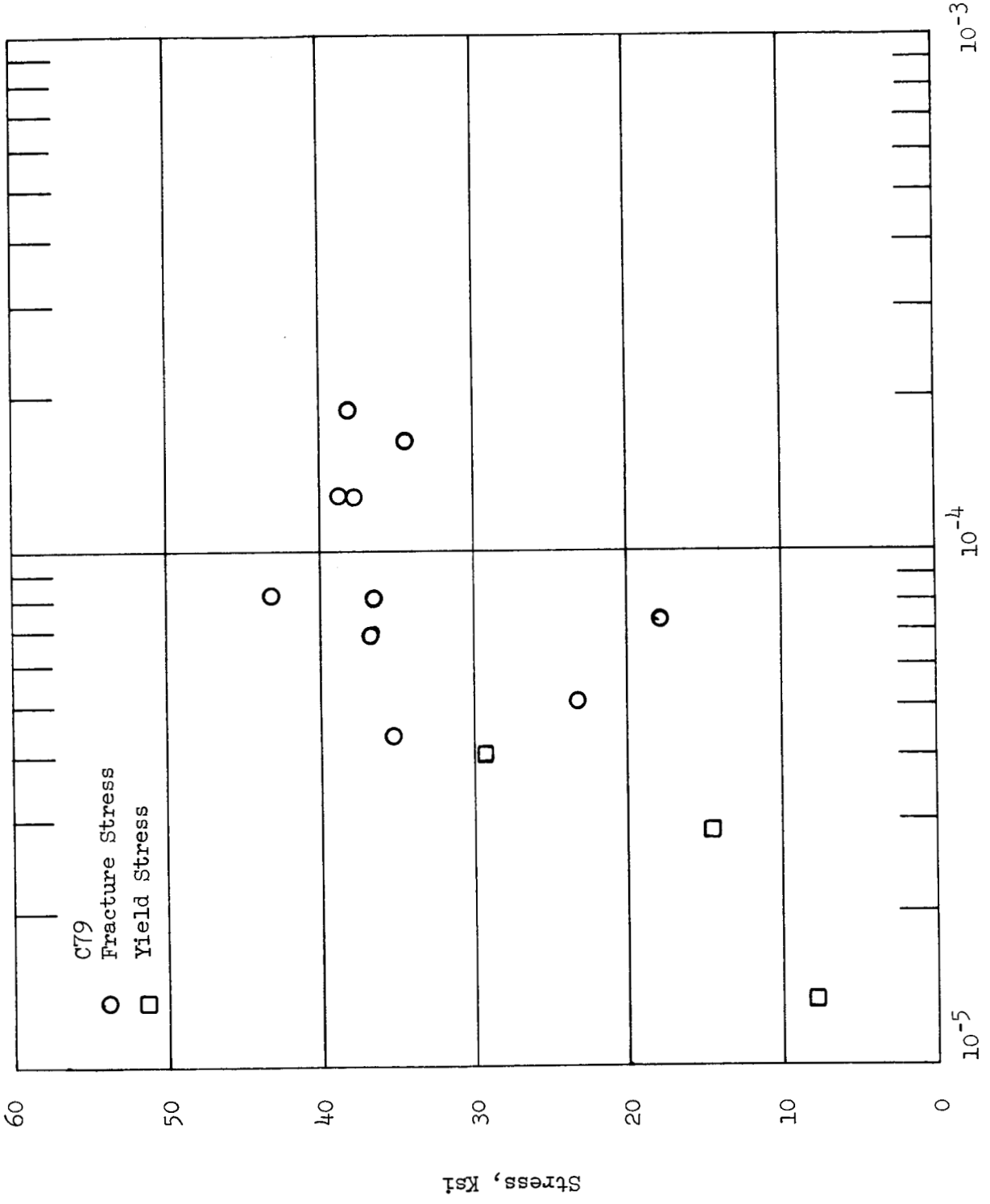

Figure 10. Effect of Strain Rate upon the Fracture Stress of Fine Grained Al_2O_3 at 1415°C.

could be seen in the tensile surface of the specimen at 4×10^{-5} sec^{-1} after the initial test, in the surface of the specimen at 2×10^{-5} sec^{-1} after the second test and in the slowest one after the third cycle.

The specimens tested above 10^{-4} sec^{-1} showed essentially no deviation from elastic behavior at fracture whereas those at lower rates exhibited increasing deviation from elastic behavior before fracture. For the latter ones the actual stresses are slightly lower than those shown. The scatter in the data preclude a determination of the strain rate effect on the fracture stresses. More data points are necessary to obtain statistical significance and calculation of the corrected stresses are required to provide accuracy.

B. Forging Experiments

Four forgings of fine-grained Al_2O_3 were done to compliment and provide guidance to the mechanical testing and to assess some of the engineering and equipment problems to be expected. Two of them were simple upset forgings which were desired to provide an assessment of microstructural effects. The other two were attempts to deep draw a 1-inch radius hemisphere from a 3-inch diameter blank. All of the forgings were done on doped Al_2O_3 preforms which had been hot pressed to greater than 99.7% density and had grain sizes of 2-3 μ.

The forgings were done in modified hot pressing equipment which have hydraulic presses. All of the punches, dies and load train were graphite. The mechanical testing has indicated that cracking and fracture are extremely sensitive to strain rate. It is important then that the punch speed be controlled during the run to provide the desired speed. Since most of this type of equipment is load controlled this requires some modification of existing operating techniques to achieve this condition. These early forgings were desired in part to provide experience in this type of operation and to identify any other problems.

The two upset forgings were done in a modified hot pressing apparatus arranged so there was no side constraint on the pieces. Both tests were done at 1450°C with a target strain rate of 4×10^{-5} sec^{-1}. These conditions are similar to those in which the bend testing has indicated highly rate-sensitive deformation resulting from GBS. This temperature is also low enough that rapid grain growth is not expected.

One of the pieces was forged to 16% height reduction and had a nominal L/D ratio of 0.72 at the end. This required a pressure of about 5,000 psi by the end of the stroke. This piece had no visible damage after forging. The second piece was forged to a reduction of 38% and required a pressure of about 8,100 psi by the end; it had a final L/D ratio of 0.63. Because of differences in initial grain size, die facing materials, and aspect ratio, the difference in pressure between the two is not an indication of strain hardening.

The 38% forging was somewhat assymetric because of corner hang-up on one side. Examination of the surface revealed several small cracks on the sides, examples of which are shown in Figure 11. These cracks originated in small regions containing several large grains. These large grains were

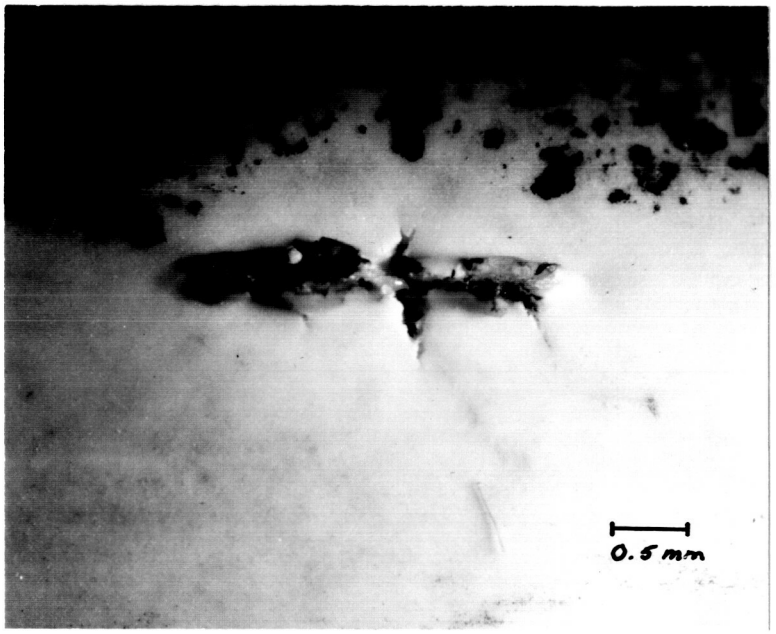

#2568-1 20X

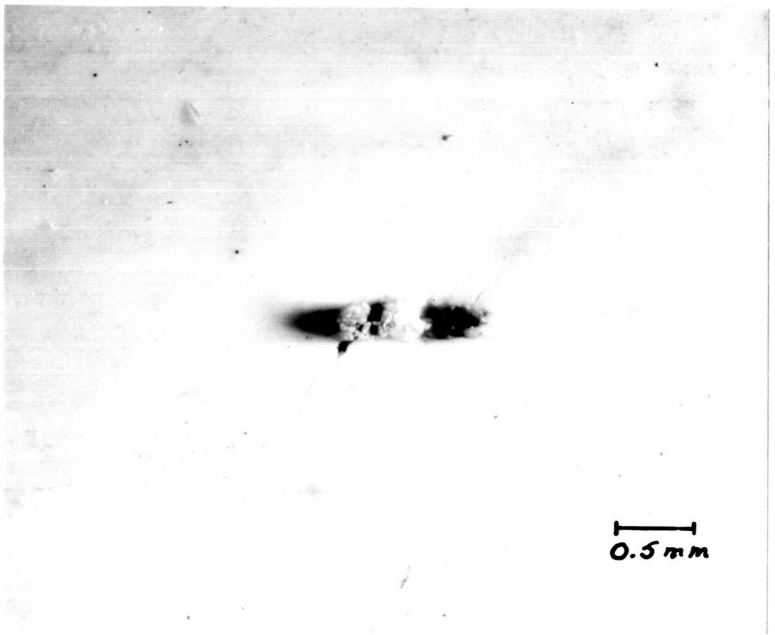

#2568 20X

Figure 11. Small Cracks Seen in the Side of Specimen JC-1474 After Forging to 38% Height Reduction. The Cracks are Associated with Small Patches of Coarse-Grained Material which are Seen to have been Extruded out of the Surface.

extruded out from the surface as can be seen in the photographs. It is at least rather encouraging that the cracks did not propagate far from the defect areas.

The initial attempt to deep draw a hemisphere was at 1500°C with a target strain rate of 4×10^{-5} sec^{-1}. A hot pressed preform of 0.080 inch thickness and 3 inch diameter was used; it had a 3 μ grain size. The punch and die were both graphite and had a coating of BN to provide lubrication and separation; the die had a 40° entrance angle. Several problems in maintaining the necessary control of the travel rate and load were indicated during the run. The piece was broken into several pieces; examination indicated that the probable cause of cracking was excessive stress or strain rate. It is thought that this was aggrevated by fluctuations of the strain rate above the nominal.

The second attempt was with a similar preform and tooling, except that the punch face was not lubricated to reduce sticking during drawing. It was run at the same nominal strain rate, but the temperature was increased to 1625°C since the starting grain size was 3 μ. The piece was not broken; however, as seen in Figure 12, there were some tears in the surface of the apex and some small cracks on the inner surface especially near the skirt where the bending had been most severe. The thinning strains were measured and found to be about 7.4% at the apex and a maximum of nearly 10% about 1/2 inch away from the apex; at the outside thickening occurred with about 6.2% at the corner and about 7.4% in the skirt. The dark spots seen on the outside surface were "hard" areas which did not deform and now stand proud of the surface, frequently with a thin area surrounding them; the cause of this has not been identified. The results of these initial forging attempts were encouraging even though some tearing and separation at grain boundaries (see next section) occurred. Substantial reductions were indicated to be feasible at relatively low temperatures, e.g., 1450°C, and it was indicated that hemispheres could be drawn at modest temperatures. It is thought that using finer grained starting materials and optimizing the travel schedule should allow successful drawing of hemispheres at relatively low temperatures.

C. Microstructural Evaluation

Microstructural examination of the bend specimens and upset forgings was done in order to evaluate deformation mechanisms and causes of fracture. Although some light microscopy was done, most of the work was electron microscopy of replicas because of the fine grain sizes; the as-deformed surfaces were extensively investigated and this was augmented with examination of polished and etched sections. A standard double replication and shadowing technique was used to prepare all replicas examined. Finally, an x-ray diffraction measurement of crystallographic orientation was performed for one of the forged pieces.

1. Deformation Features

The as-deformed surfaces were examined for many of the bend bars, and for two specimens, replicas were taken after each bend cycle. These revealed many interesting features providing evidence of sliding of grain boundaries and also some evidence of slip. There were some differences among

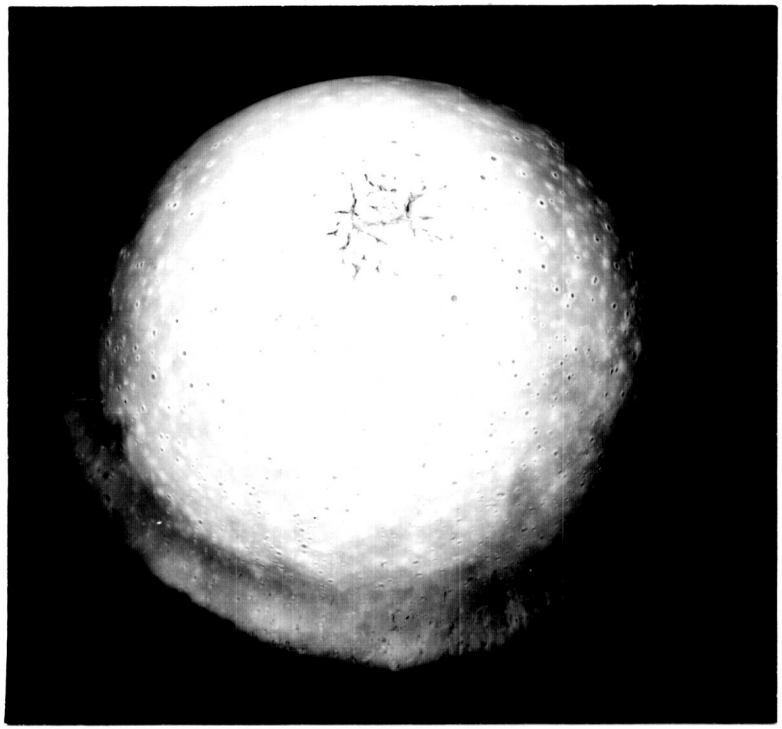

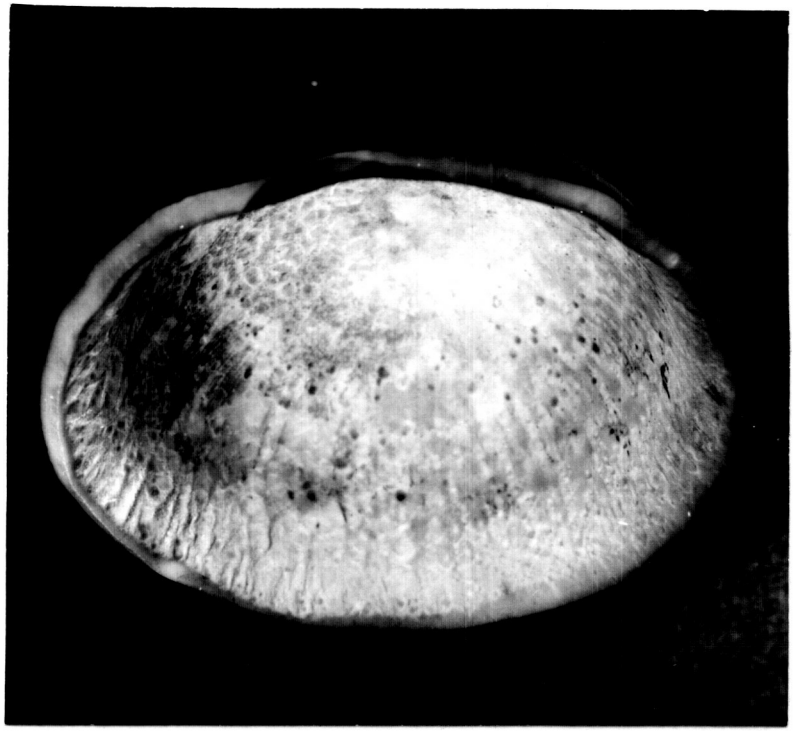

#5327-1 (a) 3/2X #5327-2 (b) 3/2X

Figure 12. Top and Bottom Views of Deep Drawn Hemisphere, D-1442 of Al_2O_3.

the various bars which suggested that the degree of surface etching and retention of features was sensitive to the vapor species in the furnace atmosphere.

In the multiple bending tests, the tensile surfaces generally took much longer to develop deformation surface features than did the compression ones. The tensile surfaces appeared only slightly different than untested, thermally etched samples for the first few cycles whereas the compression surfaces were extremely irregular even after the first cycle. After subsequent cycles, the faces began to look more similar; however, the compressive surfaces always exhibited more surface features (thermal etching excepted) and more irregular boundaries. Examples of this from Specimen FLUX-33 can be seen in Figures 13 and 14. The causes of these differences are not fully understood; it is thought possible that differences in the atmosphere directly at each surface may alter the rate of thermal etching. It is also possible that the differences reflect differences in behavior in tension and compression, but there is no supportive evidence for this at present.

Examination of these indicated considerable evidence of shear along the grain boundaries. Offset triple points were frequently seen and in the later stages of bending extremely distorted ones were sometimes seen such as are shown in Figure 15. It can also be seen that the boundaries were generally rather wavy, sometimes were even corrugated; at higher deformations, the boundary regions often appeared wide and rather indistinct suggesting extensive shear and migration. It is thought that extreme triple point distortions, such as those seen in Figure 15a, may be more likely to occur as a result of alternating strain than in unidirectional strain. Some of the irregularity of the compression surfaces were caused by rotation of grains out of the surface by boundary sliding.

Polished and etched sections exhibited similar features indicative of boundary sliding. As seen in Figure 16, for specimens prepared both by mechanical and chemical polishing, distorted triple points and boundary corrugations were in evidence. In addition wide or 'double' boundaries were frequently seen. As seen in these figures, most of the boundaries do not generally appear as badly distorted as suggested by the surface replicas. It is thought that contamination of the surface from the furnace atmosphere may have resulted in pick-up of material which inhibited boundary migration thus reducing the rate of recovery of these high energy features.

The upset forged pieces revealed many features similar to those found in the flexure specimens. Examples are shown in Figure 17 of cross sections from pieces upset 16% and 38%. Offset and distorted triple junctions can be seen in each as well as the 'double' boundaries. In the piece forged to 38% reduction some evidence of microstructural textures was also evident as can be seen from the elongated appearance of the grains in Figure 18.

The cause of these 'double' boundaries is not fully understood, but they are thought to be related to the localized shear resulting from boundary sliding. It is possible that they are dislocation networks or low angle boundaries; transmission electron microscopy should provide insight into this problem.

#691009 (a) 7500X

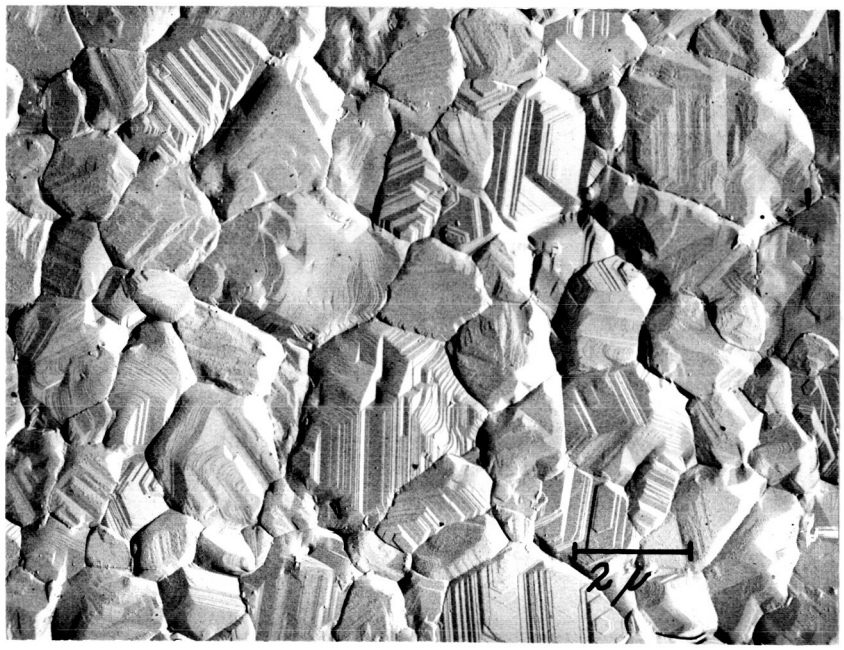

#691015 (b) 7500X

Figure 13. Compressive and Tensile Surfaces After the 1st and 2nd Cycles, Respectively, for Specimen FLUX-33.

#691049 (a) 7500X

#691043 (b) 7500X

Figure 14. Compressive and Tensile Surface After the 6th Cycle for Specimen FLUX-33.

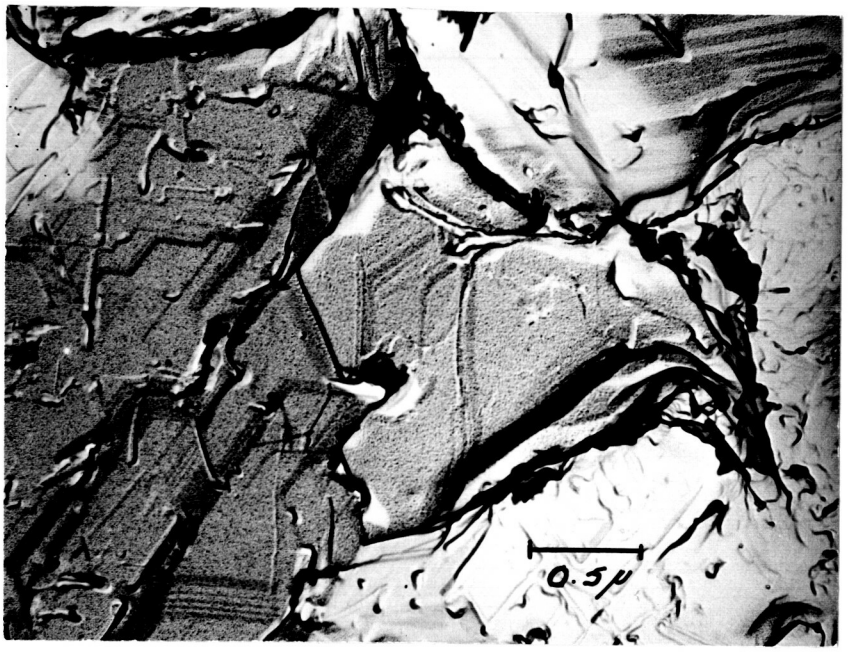

#69948 (a) 30,000X

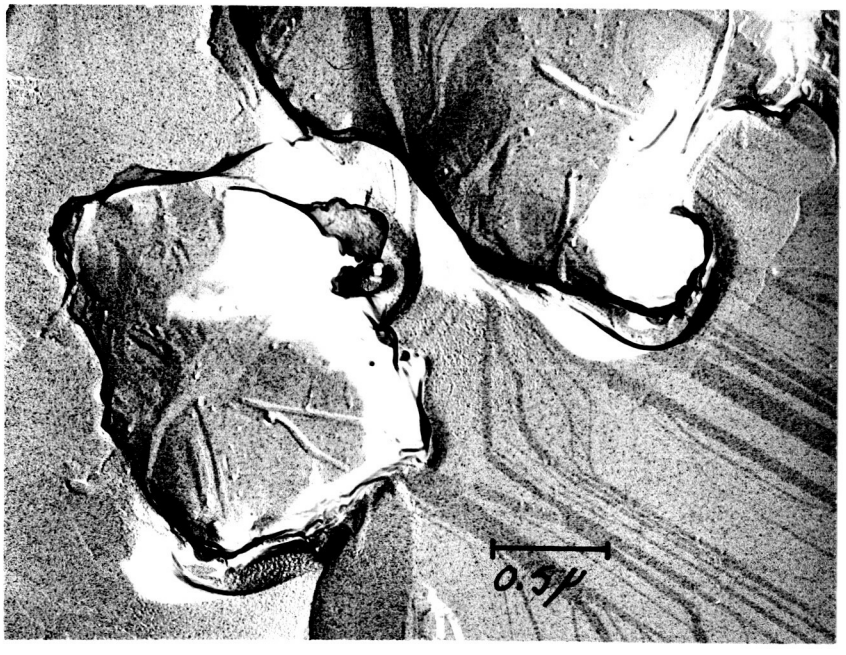

#691048 (b) 30,000X

Figure 15. Surface Replicas Showing Distorted Boundaries and Triple Grain Junctions. The top figure (a) is from the compressive surface of FLUX-32 after the third cycle and the lower is from the tensile surface of FLUX-33 after the sixth cycle.

#70254 (a) 30,000X

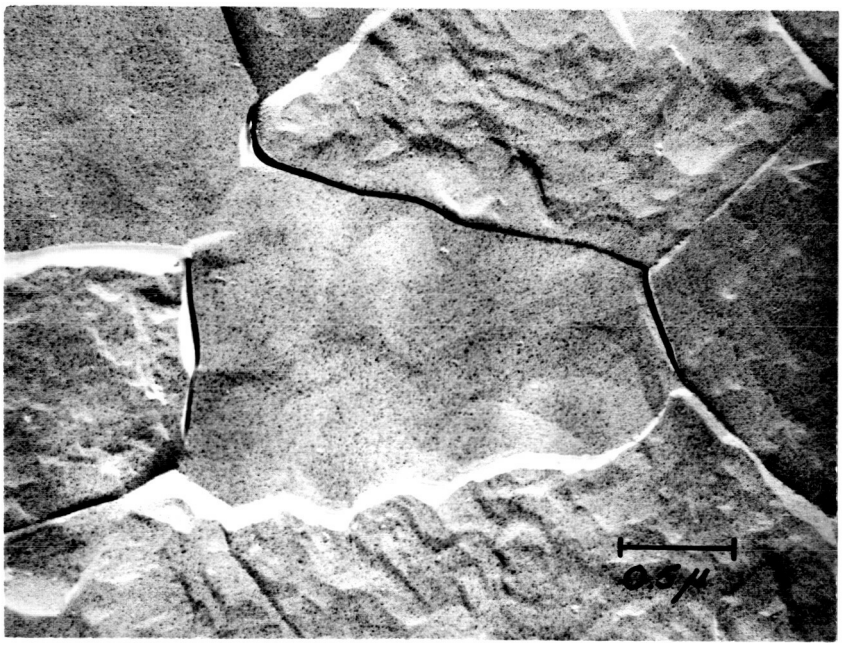

#70262 (b) 30,000X

Figure 16. Polished and Etched Cross-Sections from Specimen FLUX-30 Showing Distorted Boundaries and Triple Junctions. The top section (a) was mechanically polished and etched (H_3PO_3). The lower section was chemically polished ($Na_2B_4O_7$) and then etched (H_3PO_3).

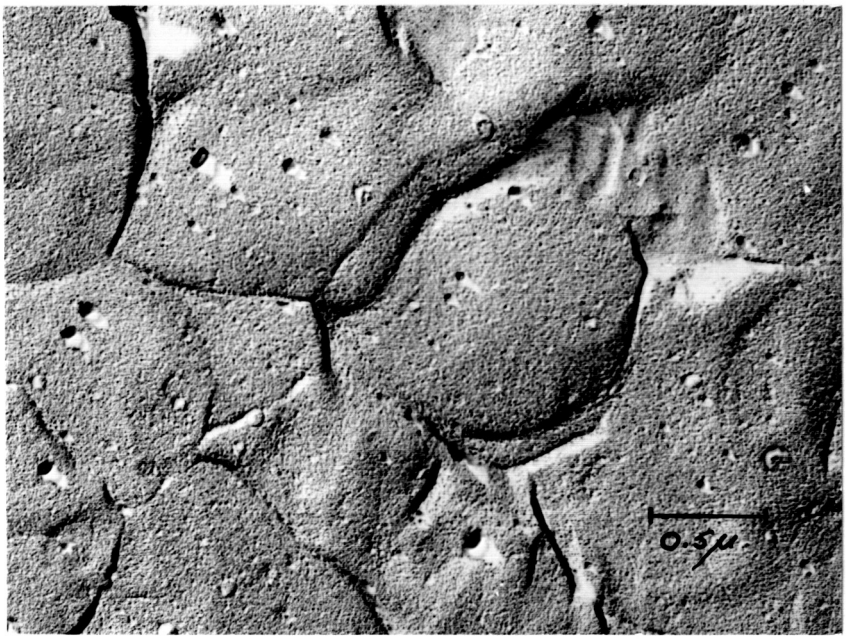

#70401 (a) 30,000X

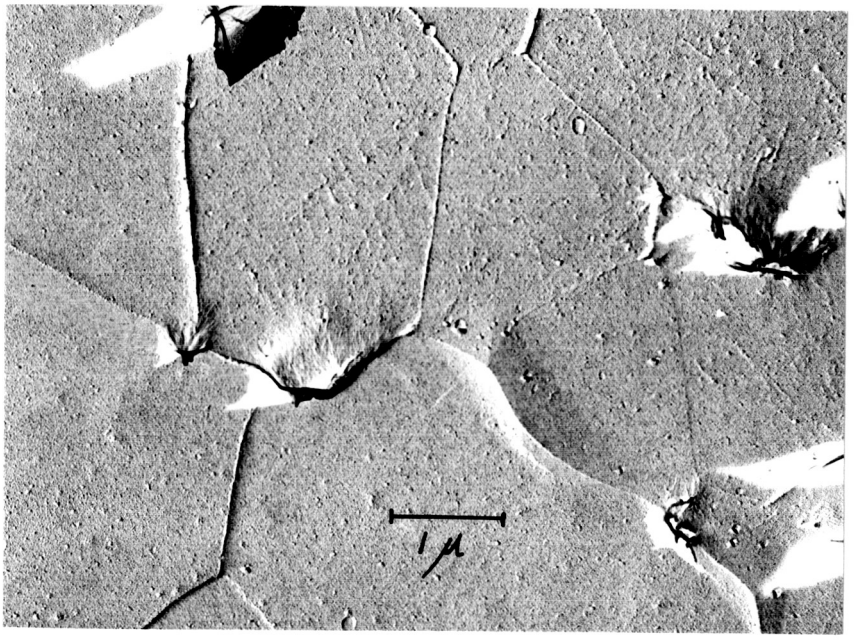

#70408 (b) 15,000X

Figure 17. Microstructures Showing Deformation Features in Samples JC-1469 and JC-1474 Forged to 16% and 38% Reduction at 1450°C. The plane of the cross-section is parallel to the forging direction for both. Specimen JC-1469 was chemically polished ($Na_2B_4O_7$) and etched ($K_2S_2O_7$); specimen JC-1474 was mechanically polished and etched (H_3PO_3).

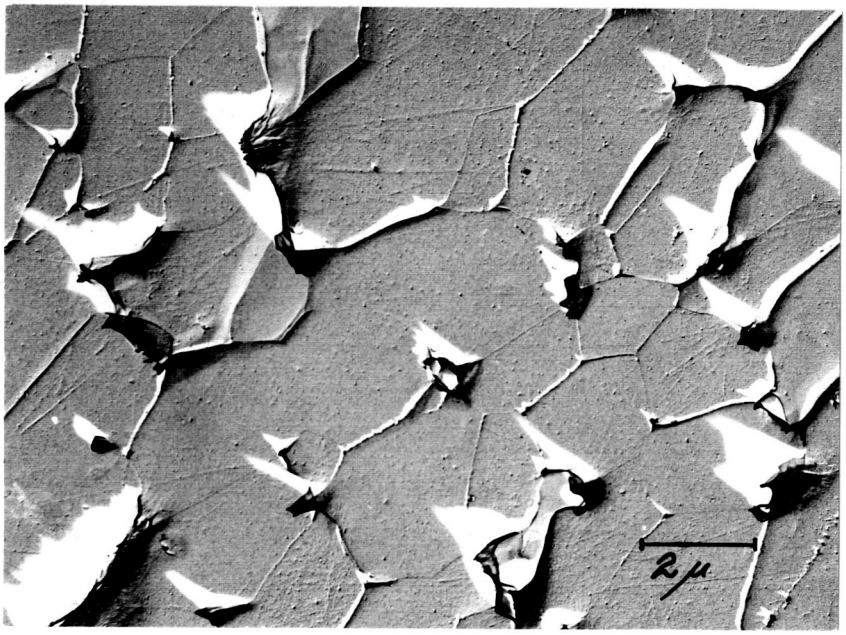

#70407 7,500X

Figure 18. Cross-Section of Specimen JC-1474 Forged to 38% Reduction Showing Microstructural Texture. Specimen mechanically polished and etched (H_3PO_3). Cross-section is parallel to the forging direction.

There were several indications of slip in the surface replicas; however, this was much less abundant than the evidence for boundary sliding. This is not surprising in view of the relative ease with which surface steps and similar evidence of slip bands can be removed by thermal etching of the surface or by grain boundary migration. Some evidence was seen, however, of surface steps which were extremely suggestive of slip band emergence. Examples of this from the compression surfaces of two specimens are shown in Figure 19. Figure 15a shows some similar steps and in addition has a boundary with two sharp steps in it; these are suggestive of a slip band, boundary intersection. Finally, protrusions were sometimes seen extending out of a grain and penetrating into the adjacent one; an example of this is shown in Figure 20. These are also suggestive of the emergence of fine slip bands and their penetration into neighboring grains.

Direct evidence of slip in the polished and etched sections is more difficult to obtain. Usual etch pit techniques give etch pits which are larger than the grain size of the present material. Several different etches and conditions were used here to attempt to being out pits or indicate dislocation networks. Under some conditions light lines were seen in grains, see for instance Figure 17a, and at high magnification these often have small pits along them, as can be seen in Figure 21. In addition, there is often a small jog in the boundary where such lines intersect it. It is thought likely that these lines are traces of dislocation arrays or networks. It should be noted that this specimen was chemical polished and etched without any mechanical grinding so that no polishing damage would be induced.

2. Cavitation and Cracking

The occurrence of cavitation at grain boundaries, particularly at triple points was evident during examination of these specimens. This has, of course, been frequently observed in creep tests of the oxides. Examples of these can be seen in Figure 22 which is a cross-section of a multiple bend specimen after 38% total strain in five cycles; although this region had a high density of cavities they were certainly not found at all of the grains indicating that considerable sliding can occur without cavity formation.

The specimen forged to 38% reduction exhibited a considerable amount of separation at triple points as can be seen in Figure 18. The specimen which received only 16% reduction exhibited relatively little separation of this type. The two pieces were taken from different billets so it is not certain that the difference is entirely a result of the increased strain. Comparison of this forged specimen with the multiple bend specimens indicated that cavitation was more extensive after unidirectional straining than after alternate straining. Examination of two specimens forged on a previous program,[8] to 35% and 37% reduction at 1425°C and at a somewhat higher rate revealed many essentially similar features, including grain elongation, with the exception that there was very much less intergranular separation. These two specimens had lower L/D ratios, about 0.27, which results in a significantly higher frictional constraint and effectively produces a hydrostatic pressure.[54] Comparison among the various specimens suggests that the amount of cavitation is worse for unidirectional than alternating strain and is decreased with increasing hydrostatic compression; it is presumably most severe in tension.

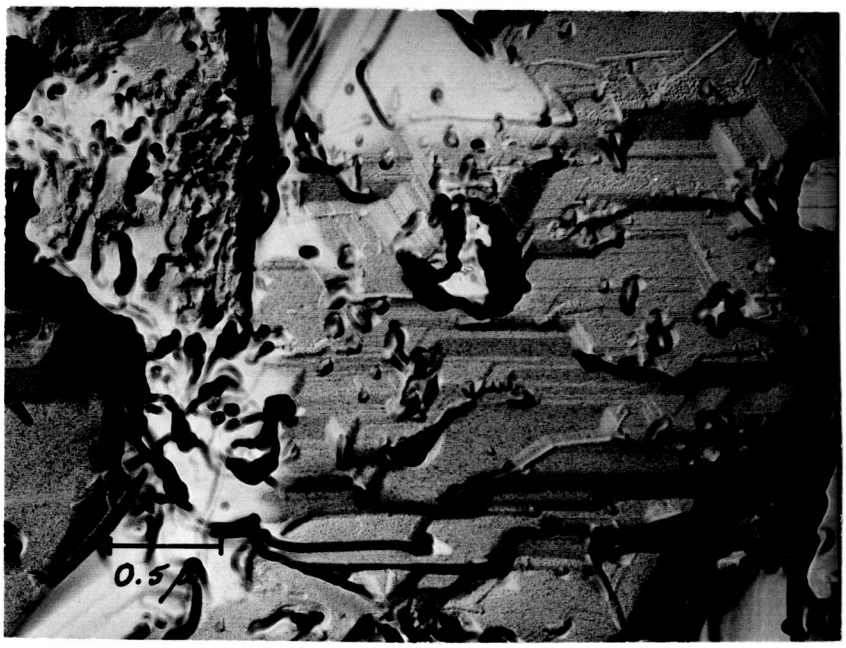

#69946 (a) 30,000X

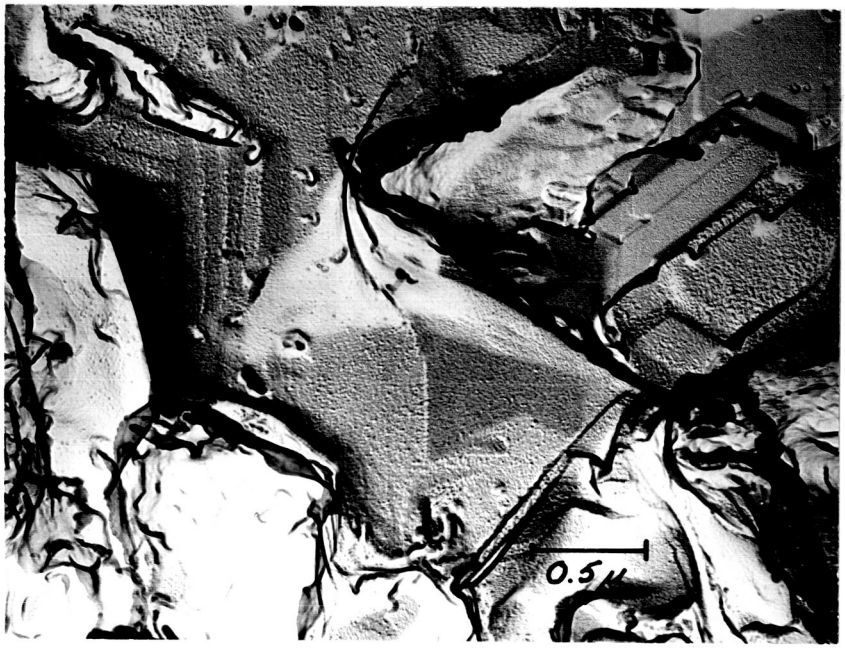

#691053 (b) 30,000X

Figure 19. Fine Surface Steps Seen Primarily on Compression Surfaces which are Suggestive of Fine Slip Bands. The top figure is from the compression surface of FLUX-32 after the third cycle; the lower one is from the compressive surface of FLUX-33 after the sixth cycle.

#691057 30,000X

Figure 20. Protrusions at a Grain Face Extending into a Neighboring Grain. Tensile Surface of FLUX-33, 6th cycle.

#70405 45,000X

Figure 21. Microstructure from Specimen JC-1469 Showing Faint Lines and Pits Which are Thought to be Traces of a Dislocation Network. Note the grain boundary is slightly jogged where the line intersects it. The specimen was chemically polished ($Na_2B_4O_7$) and etched ($K_2S_2O_7$).

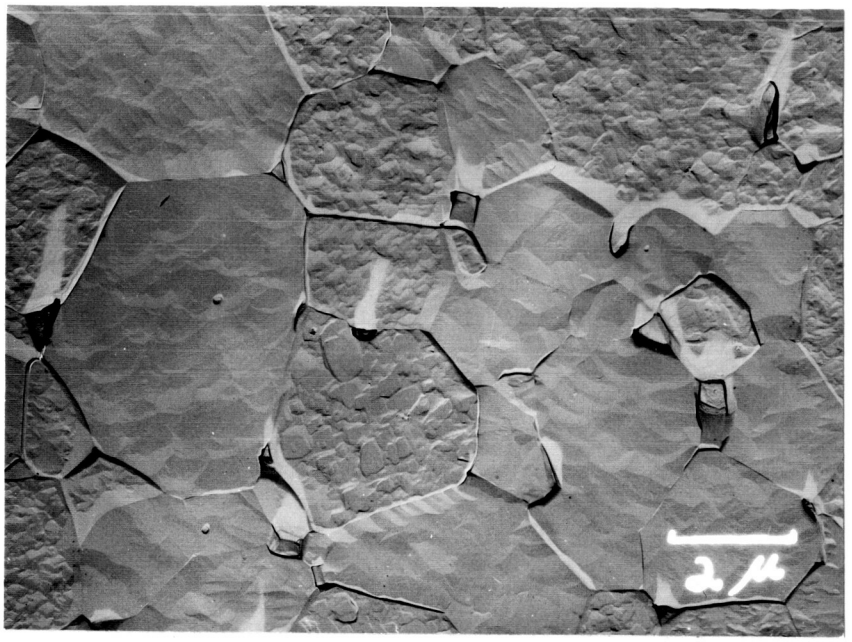

#70284 7500X

Figure 22. Microstructure of Specimen FLUX-30, Which Broke in the 5th Cycle, Showing a Region with a High Density of Grain Boundary Cavities. Chemically polished ($Na_2B_4O_7$) and etched (H_3PO_3).

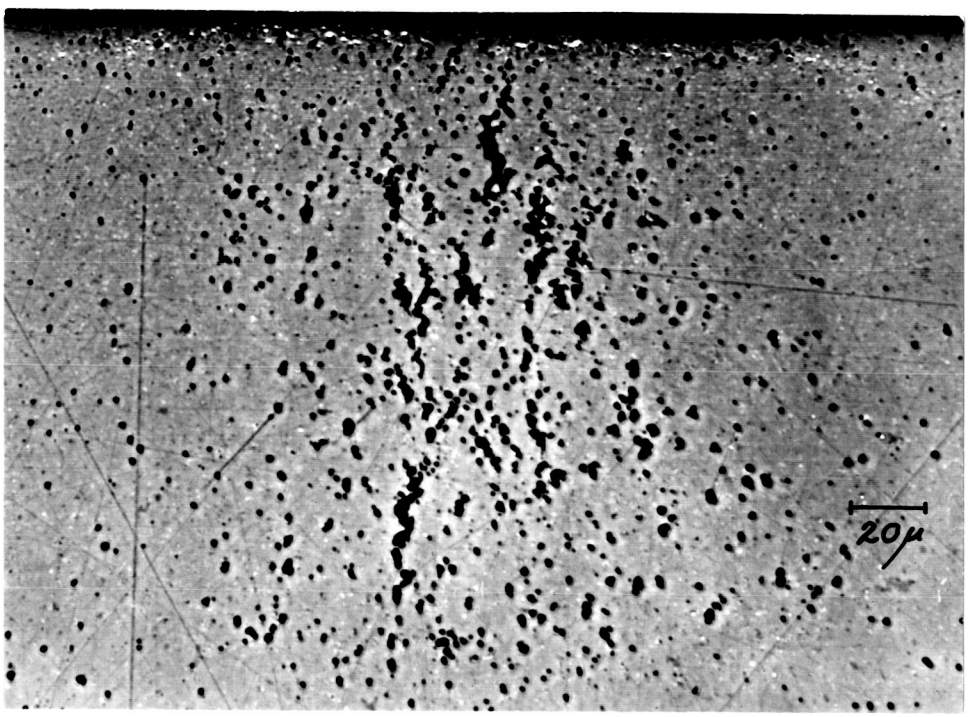

#5268-2 500X

Figure 23. Intergranular Cracking in Specimen FLUX-32, After Four Bend Cycles.

In examination of the multiple test bars, patches were seen which had a much higher than average density of intergranular cracks. An example of this is shown in Figure 23. When testing was discontinued on this specimen, there were no visible cracks in the surfaces; it can be seen that this region is very nearly to the point that a visible crack would develop. A presumably similar occurrence can be seen in Figure 4 in the development of the small cracks. The development of these small cracks was often observed in regions which were initially identifiable by a discolored spot (sometimes darker, sometimes lighter); it is thought likely that pore nests or impurities or both are often responsible for the initiation of these cracks. This suggests that the strain limitations in many of the multiple bend bars was a result of initiation and growth of cracks in initially defective areas.

3. Crystallographic Texture

To gain an additional indication of the contribution of slip to the deformation, the specimen forged to 38% was analyzed for preferred crystallographic orientation by an x-ray diffraction technique which has been developed and used on previous programs.[9,55] The crystallographic texture can be described by what is essentially an azimuthally averaged, inverse pole figure. In this procedure the relative population density of different planes is plotted against the angle between these planes and the basal (000.1) plane. With proper normalization this is then also a plot of the population density of the basal planes at the same angle from the reference surface.

Experimentally, the procedure is simple. The diffraction pattern of a randomly oriented (powder) sample is obtained. Values are calculated of $P_o(hk{\cdot}l)$ defined by the relation

$$P_o(hk{\cdot}l) = \frac{I\,(hk{\cdot}l)}{\sum_{hkl} I\,(hk{\cdot}l)}$$

where I (hk·l) is the diffraction peak intensity for reflection from the (hk·l) plane. Similarly, the diffraction pattern of the forged body is obtained using a face perpendicular to the pressing direction. Values of P (hk·l) are calculated as before, and then the ratios $R(hk{\cdot}l) = P\,(hk{\cdot}l)/P_o$ (hk·l) are calculated. These values of R are plotted against θ, the angle between the plane hk·l and 00.l.

In the case of a random (powder) sample, R has the constant value of unity. In the case of a perfectly oriented sample, R is zero everywhere except at $\theta = 0$ where it has some large finite value. In the case of a distribution of orientation R will, in general, decrease monotonically from $\theta = 0$ to $\theta = 90^{\circ}$. The better the alignment of the crystallites, the greater will be the intercept at $\theta = 0$ and the steeper the drop with increasing θ.

The specimen had a marked basal texture as shown in Figure 24. This type of crystallographic texture has been reported previously for alumina forged at much higher temperatures,[2a, 10] and is strong evidence of basal slip. The orientation of the 'c' axis parallel to the forging direction has also been reported for the hcp metals in which the basal slip system is the most easily activated.[56] These results indicate that even at 1450°C in fine grained material, basal slip provides a major contribution to

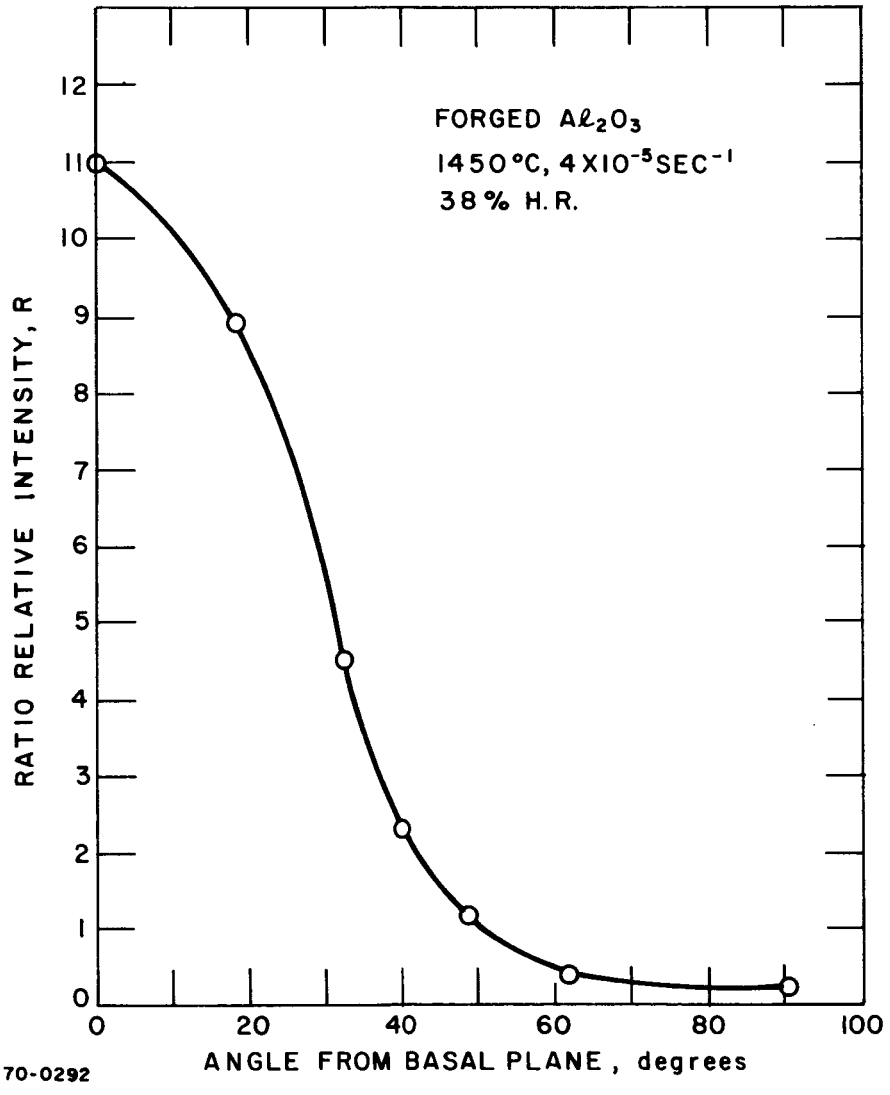

Figure 24 RATIO OF RELATIVE X-RAY INTENSITY FOR SPECIMEN JC-1474 FORGED 38% SHOWING STRONG BASAL TEXTURE.

deformation. It should be emphasized that this forging was done under conditions of relatively low temperature and strain rate where the highly rate-sensitive deformation has previously been attributed to grain boundary sliding[25] or diffusional creep.[29,30,44]

IV. DISCUSSION

The present results provide substantial evidence to indicate that deformation in fine-grained Al_2O_3 occurs by GBS. The change in macroscopic flow parameters such as the reduced rate sensitivity, indicate a change in behavior from diffusional creep to a non-Newtonian process at very fine grain sizes. Microscopic evidence, such as offset and distorted triple junctions, and wavy, distorted or indistinct grain boundaries provide strong indication that the deformation is dominated by boundary sliding. Further, there are indications that slip plays a significant part in the accommodation process. Finally, some additional questions, such as the effects of atmosphere and purity, have been raised for which answers have not yet been found.

The microscopic features observed, such as the surface steps and sharply jogged boundaries seen in the multiple bend specimens, and the occurrence of a strong basal texture, in a forged sample, provide evidence that slip participates in the grain shape change process. The strong crystallographic texture indicates not only that basal slip occurs, but that it is the preferred system; this is not surprising in view of its relative ease of activation in sapphire in comparison with other slip systems. The contribution of slip in this fine-grained material has previously been questioned because no obvious increase has been observed in the dislocation density after straining; it is now argued that this condition is not unexpected because of the relative ease of annihilation of dislocations at the grain boundaries in these fine-grained materials.

The other principal reservation about the occurrence of slip is that the flow stress of the fine-grained materials is low compared to that for slip in sapphire. In order to facilitate such a comparison, flexural flow stress data for polycrystalline materials at two different grain sizes are plotted versus temperature in Figure 25, along with upper yield stress data for slip in several modes in sapphire; all data are to a tensile strain rate of 4×10^{-5} sec^{-1}. Data for the tensile,[57] and the compressive[58] yield stresses for basal slip in sapphire are shown; the tensile stress for a nominal 60° orientation is used. The scatter in the compressive yield at lower temperatures is due to concurrent twinning. In addition, the upper yield stress for compression of 0° sapphire, which resulted in slip on what was presumed to be the rhomobohedral system,[59] is plotted along with a point for rhombohedral slip in a whisker.[60] Although there is still uncertainty as to the possible non-basal slip systems in Al_2O_3, there is increasing evidence that slip can occur on the $\{\bar{1}012\}$ $[10\bar{1}1]$ system.[60,61] Also plotted is the upper yield stress necessary to activate basal kinking in compression of 90° sapphire.[59] Although this apparently requires only movement of basal dislocations,[62] it can provide deformation when the applied stress is nearly parallel to the basal plane.

It can be seen that the flow stress for the fine-grained polycrystalline material is generally lower than the basal yield stress and more than an order of magnitude below that for rhomobohedral slip. It should be mentioned that as the strain rate is increased, at a given temperature, there is no indication of a change of behavior as the applied stress increases over that required for basal yield in sapphire; this indicates that the contribution of slip remains approximately constant over the entire range of stresses and strain rates investigated. The low flow stresses have been interpreted to suggest that slip in the fine-grained polycrystalline material should not be significant;

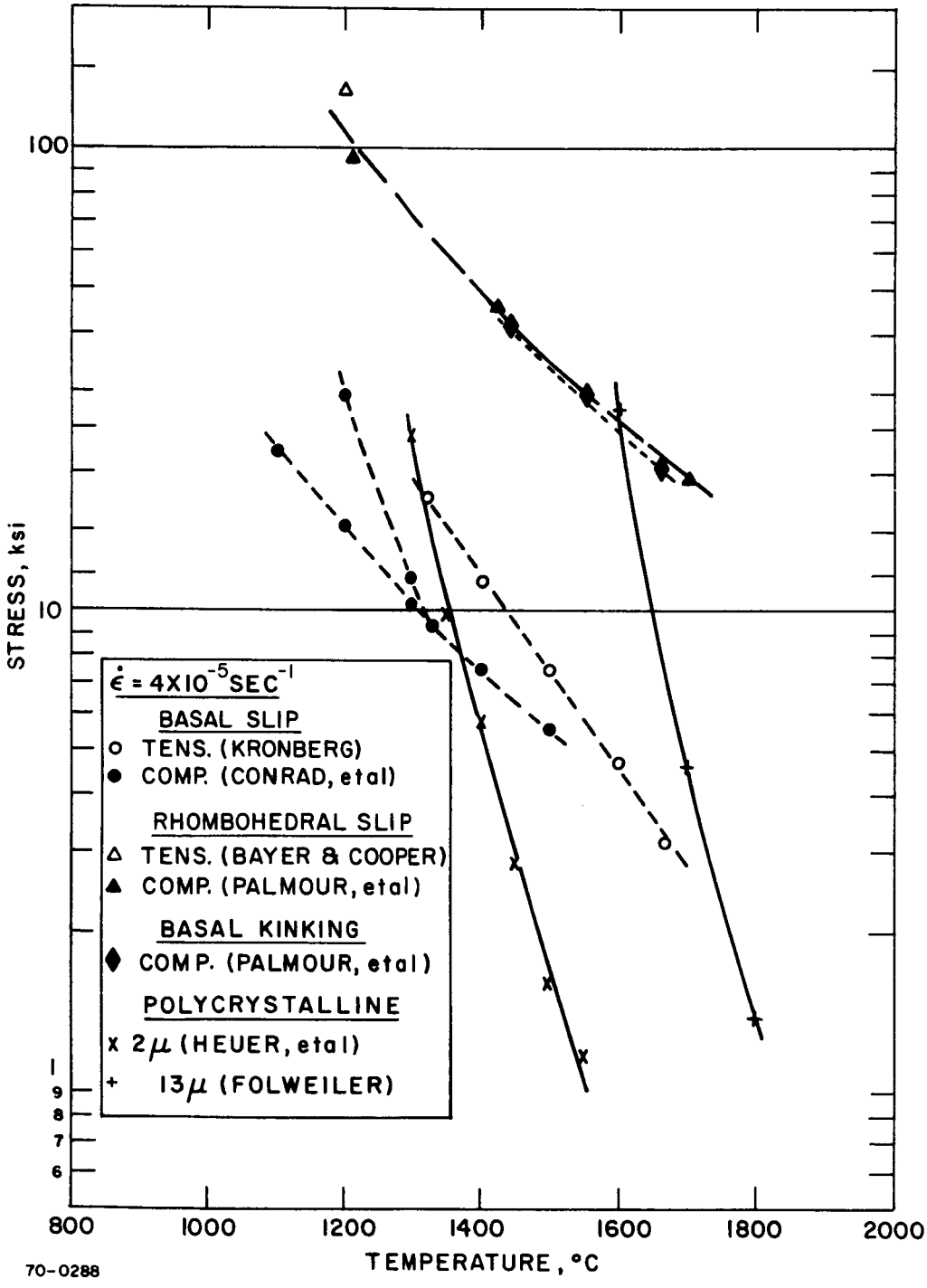

Figure 25 TEMPERATURE DEPENDENCE OF YIELD STRESS (AT $\dot{\epsilon} = 4 \times 10^{-5}$ sec.$^{-1}$) FOR 2μ, [25] AND 13μ, [29] POLYCRYSTALLINE ALUMINA AND FOR BASAL SLIP, [57, 58] RHOMBOHEDRAL SLIP, [59, 60] AND BASAL KINKING. [59]

such a conclusion cannot be accepted, however, without a greater understanding of the factors controlling the yield stress in sapphire. The sharp yield stress for basal slip in sapphire is apparently the result of the dislocation multiplication process. However, it is not certain at the present whether the stress levels measured are those required to overcome the Peierls stress with the aid of thermal activation, or are determined by a dislocation climb process.[63] If they are limited by the Peierls barrier then similar stresses would have to be developed in polycrystalline materials to activate basal slip. If, however, the basal slip, yield stress is determined by the stress necessary for dislocation multiplication, perhaps involving dislocation climb, then any feature such as GBS, which could provide an easier multiplication mechanism would allow basal slip at lower resolved stresses than in those measured in sapphire. This is not unreasonable since the lack of cross-slip in Al_2O_3 presumably requires the creation of Frank-Read sources by a process such as climb.[58,64]

Two features of deformation by GBS have been identified which may explain the occurrence of slip at these reduced stresses. The boundary sliding was shown by transmission electron microscopy, in previous work,[25] to involve the movement of dislocations in the boundaries. Recent evidence has been seen in metals to indicate not only that sliding occurs by the movement of dislocations in the boundaries, but that this movement results in the emission of lattice dislocations into the grains.[39,40] This observation, that sliding boundaries emit dislocations into the grains, coupled with earlier suggestions[65] and observations,[17] that the absorption of dislocations into a boundary can cause shear along the boundary, can be combined; and it can be postulated that the process of boundary sliding and grain shape change by slip are mutually cooperative, interdependent processes. This process would predominate at fine-grain sizes where the boundaries are the principle sources and sinks for dislocations and no significant build-up of dislocations results in the grains.

A direct comparison of applied stresses with single crystal, yield stresses is made more difficult by the development of large stress concentrations in polycrystalline bodies. Such stress concentrations obviously occur where slip bands in adjacent grains are piled up at the boundaries. When boundary sliding occurs additional stress concentrations occur at points of constraint which restrict sliding of otherwise relaxed boundaries.[49] Direct observation has been reported[66] of slip on a secondary system in polycrystalline LiF at a resolved shear stress an order of magnitude less than the single crystal value for the critical shear stress.

It seems reasonable to assume that the two factors of boundary sliding-lattice dislocation interdependence and stress concentration effects can account for the occurrence of basal slip even at stresses below the yield stress seen in sapphire. These arguments are equally applicable to rhombohedral or other non-basal systems; it seems likely that some non-basal slip must occur, particularly when necessary to provide relief at points of constraint to sliding. Some contribution to grain shape change by diffusional creep cannot be categorically ruled out from the evidence at hand. It is possible that the additional deformation, over that provided by basal slip occurs as a result of a combination of non-basal slip and diffusional creep.

Comparison of the data from the present results and previous investigators[25,29,30]

reveals a trend of reduced values of the strain rate sensitivity, m, from near unity at grain sizes in excess of 10-15 μ down to about 0.6-0.7 for grain sizes less than about 5 μ; there is a similar substantial reduction in the activation energy, ΔH, with reduced grain size (see Figure 8). These indicate a change in the controlling deformation mechanism with reduced grain size. The reduction in ΔH from 185 Kcal/mole at very coarse grain sizes to about 100 Kcal/mole at 1 μ is about that expected for a change from control by lattice diffusion to grain boundary diffusion.

The microstructural and other data indicate that this is not simply a transition from lattice to grain boundary controlled diffusional creep, however. For the fine-grained material, deformation is otherwise indicated to be by GBS; the low value of ΔH is consistent with this since the limiting features could be either movement of dislocations along the boundary or the generation and absorption of lattice dislocations at the boundaries. It is perhaps possible that grain shape accommodation by diffusional creep is the limiting feature; at these fine grain sizes boundary diffusion would probably be controlling.

In the coarser-grained materials where m values near unity were found, the deformation appears to be controlled by diffusional creep. The fact that ΔH continues to increase in this region and that the strain rate-grain size exponent appears to be in excess of 2 in the range of 7 to 34 μ[29] may be evidence of a contribution of grain boundary diffusion to the diffusional creep, or it may be a result of some contribution of GBS. It is not obvious at this time whether the sliding necessary to accommodate diffusional creep occurs by a diffusional mechanism or by a boundary dislocation mechanism.

At very coarse grain sizes the situation is somewhat ambiuous. The data in Figure 8 at 100 μ were taken from Warshaw and Norton,[30] where the deformation kinetics indicated a dislocation climb mechanism. Although not shown in Figure 25, the flow stresses were only moderately in excess of those for basal slip in sapphire and were much less than predicted from diffusional creep relations. It is suggested that creep in these specimens was controlled by basal slip, but that the extensive cracking which occurred was a result of failure of the material to satisfy the von Mises criterion because of insufficient non-basal slip. There has also been evidence reported,[6,7] to indicate that under some conditions diffusional creep may predominate even at grain sizes of 100 μ. It seems possible that either of these conditions could occur depending on the particular conditions of stress, temperature and perhaps specimen porosity.

For materials previously forged at high temperatures, considerable evidence of basal slip with relatively little cracking was reported.[2,10] Most of the specimens, however, were moderately fine grained. It is likely that the compressive constraint may have inhibited cracking and resulted in greater activation of non-basal slip systems. It is thought that the high temperature and relatively high stress and strain rates resulted in deformation which was apparently dominated by slip, rather than by diffusional creep as would be suggested by the above discussion. The reported information does not allow clear distinction of whether or not a contribution of diffusional creep occurred or whether or not boundary sliding was important. These

results do serve to point out that the transitions from one mechanism to another will be influenced by temperature and strain rate as well as by grain size.

At higher strains in the fine-grained material, an apparent strain hardening occurred in some materials. For these specimens substantial strain enhanced grain growth occurred and accounted for most of the increase in flow stress. This seems reasonable for a mechanism in which there is not a significant increase in the lattice dislocation content during straining. It is possible that as grain boundaries become more distorted, the ease of sliding may be effected somewhat resulting in some increase in the flow stress, but the data suggest this was not a large effect. Eventually the development of intergranular cracks and pores would result in an apparent weakening. The question of why strain induced grain growth occurred in only some specimens still needs to be resolved, but may be simply a result of differences in the amount or distribution of MgO in the specimens.

The present results indicate that there is a considerable effect of specimen purity, or test atmosphere, or perhaps both, on the ease of deformation. A purity effect would not be surprising since grain boundary segregation of impurities would be expected to effect the ease of sliding. An effect of test atmosphere is rather interesting; the considerable difference in strain rate observed between previous work by Warshaw and Norton,[30] and Coble and Guerard which were done in vacuo and that of Folweiler[29] and Heuer, et al[25] which were done in air could be explained by an atmosphere effect. The data are not sufficiently unambiguous, however, to allow a conclusion on this point.

Several interesting observations were made on the process of crack formation; however, there is as yet insufficient information to allow identification of the mechanisms of crack iniation and growth. Cavities developed at triple points as a result of grain boundary sliding and it can be expected that any factors which allowed more extensive grain boundary migration or easier grain deformation would reduce this.[68,15] It can be expected that any residual gases in the hot pressed bodies would enhance the formation and growth of intergranular cracks and prevent their closure during annealing; this consideration makes the question of carbon content very important since it is expected to be present as CO. Most of the actual macroscopic cracks observed were thought to have originated as a result of inhomogeneities in the materials, such as pore nests, large grain patches, or even impurity sites; elimination of these starting defects would obviously be beneficial. The data indicated that the initial appearance and subsequent growth of these cracks was more rapid at higher strain rates and commensurately higher stresses.

Taken together the deformation and fracture results from mechanical tests and the forgings indicated that forging of fine-grained Al_2O_3 at moderate temperatures is feasible. An adequate capacity for strain seems to exist in the fine-grained material; success in understanding and preventing intergranular separation seems to be the eventual limiting feature. At present, however, the elimination of defects in starting materials would provide an increased capacity for strain. The indications are that there is a greater capacity for strain in compression, but that even in tensile modes useful forging is possible. The mechanical test results confirmed that adequate analysis and control of the strain rate during forging will be extremely important.

V. SUMMARY AND CONCLUSIONS

An investigation into the deformation behavior and fracture of fine-grained Al_2O_3 was performed in order to provide both mechanistic understanding and useful data for application to the forging of ceramic oxides and of Al_2O_3 in particular. This system was selected for study in part, on the basis of an extensive review of the literature on the deformation of oxide ceramics. The principal effort for this year has been on mechanical testing of fine-grained Al_2O_3. A series of multiple bend tests were performed on 2 μ Al_2O_3 at 1415-1450°C to allow assessment of the effects of deformation to large accumulated strains. In addition, a series of tests were done on 1 μ and 15 μ Al_2O_3, over the range of 1250-1750°C to further clarify the stress-strain rate-grain size relations. This group of tests confirmed that at very fine grain sizes a transition to a non-Newtonian deformation mechanism occurs. Additional information on the grain size dependence could not be obtained because of an unexpected, and as yet unexplained, effect of either test atmosphere or specimen purity. Finally, an investigation of the effects of strain rate on fracture stress was initiated.

In order to evaluate the multiple bending experiments, which involved bending to an outer fiber strain in excess of 5%, an analysis was performed of the effects of curvature and large deflections on the four-point bend test. The results indicate that at high deflections the combined effects of the horizontal load component at the load supports, and the friction at the load supports have a substantial effect on the actual bending moment; depending upon the coefficient of friction the actual applied bending moment can be either larger or smaller than that indicated by the simple calculation. Further, these effects are substantially changed upon reversal of the bending moment.

A few forgings were done to complement the mechanical testing and to provide an indication of the engineering problems to be anticipated. Two upset forgings were done on 2 μ Al_2O_3 preforms at 1450°C; these were used for further microstructural analysis. Two deep drawn hemispheres were attempted at 1500 and 1625°C with 3 μ Al_2O_3; one of these survived intact but exhibited some cracking. These forgings provided valuable experience in satisfying several of the engineering requirements such as strain rate control and specimen lubrication.

Extensive microscopic examination was conducted on the mechanical test specimens and the upset forged specimens. Extensive evidence for grain boundary sliding such as offset triple points, distorted grain boundaries and triple point voids, was seen in these specimens. In addition, evidence of slip including surface steps and the development of a strong basal texture was observed. Finally, strain enhanced grain growth was found in some of the multiple bend specimens. Observation indicated that the limiting cracks in the specimens tested here were generally formed at defective or inhomogeneous areas in the specimens.

On the basis of the results and analysis presented here, the following conclusions are warranted:

1. A transition in deformation mechanism occurs in Al_2O_3 at grain sizes below 5 μ to a non-Newtonian, grain boundary

sliding mechanism which is thought to involve the movement of dislocations in the boundaries.

2. There is substantial evidence to indicate that the grain shape change process involves a significant contribution of basal slip. The relative contributions of non-basal slip and diffusional creep to the accommodation process cannot yet be established.

3. Under conditions where grain growth occurred during tests, the rate of growth was significantly enhanced by concurrent strain and resulted in an appreciable increase in the flow stress at constant strain rate. The differences in test conditions or specimen chemistry which allow grain growth under some conditions and not in others have not been identified.

4. A substantial effect of either test atmosphere, specimen purity or both on the deformation rate was observed. At present it is not understood which of the two possible causes was dominant; the results have sufficient consequences to subsequent forging work to justify further investigation of this area.

5. In the present work, microscopic cracks seemed to form at defective areas such as pore nests, large grain patches, or high impurity sites. The growth of those cracks, to the point at which unstable propagation resulted, occurred faster at higher strain rates and the commensurately higher stresses. In addition to these larger cracks, damage as a result of grain boundary cavitation was also observed.

6. There is sufficient ductility in very fine-grained Al_2O_3 to allow substantial forging in both the tensile and compressive modes. Control of the strain rate is extremely important for this material and elimination of defects in the preforms would allow greater strains before cracking becomes serious.

VI. APPENDIX

Analysis of Flexural Test Data

The non-linearities in the stress distribution through the cross-section which occur in the plastic bending of beams result in deviations of the outer fiber stress from that calculated from the usual elastic formula. The use of a more exact expression for the determination of the stress from the measured bending moment curves is, therefore, desirable. A useful technique for making this correction, which allows treatment of an arbitrary stress distribution in a plastically bent beam, has been previously developed.[69] However, bending to larger strains, especially in the multiple bending experiments, indicated that the possible influence of several additional effects, resulting primarily from the large deflections, required further consideration. A discussion of the several areas considered follows with emphasis on those which appear to be the most influential on the present tests. The possible deviations can be categorized into three broad areas with significant effects coming from each under some circumstances.

A. Stress Distribution in the Beam

As mentioned, a technique has been developed which allows the determination of the outer fiber stress in plastic bending.[69] This technique requires that a series of constant rate tests be performed over a range of bending rates. The outer fiber stress is given by the relations:

$$\sigma = \frac{2M}{bh^2}\,(2 + n_b + m_b) \qquad \text{(A1)}$$

$$\text{where} \quad n_b = \left(\frac{\partial \ln M}{\partial \ln \varphi}\right)_{\dot{\varphi}} \; ; \; m_b = \left(\frac{\partial \ln M}{\partial \ln \dot{\varphi}}\right)_{\varphi} \qquad \text{(A2)}$$

where M is the bending moment; φ, the included angle of bending in the gage section; $\dot{\varphi}$, the rate of bending and b and h are the specimen width and depth. The values n_b and m_b are determined graphically over a range of strains and strain rates. This data is then used to generate a family of stress-strain curves over a range of strain rates. This has the advantage of allowing determination of the stress during the approach to steady state and of accounting for strain hardening effects. The method allows the consideration of arbitrary stress, strain, strain rate relationships rather than requiring simplifying assumptions about the strain or strain rate dependence.

The above expression does not take into account the effects of curvature of the beam on the stress distribution. It is well known that in highly curved beams a radial stress develops and the circumferential stress becomes nonlinear. The elastic solution to this is well known; this has also been treated for plastic yielding assuming the maximum shear stress (Tresca) yield criterion.[70] The problem has not, however, been treated for a more general yield condition which allows the possibility of a strain rate sensitive and/or strain hardening flow stress. This simplified plastic analysis indicated that the effects are still small at the curvatures found here (i.e., equivalent to an outer fiber strain of 5%); for instance,

at this curvature the moment at yielding is 97% of that calculated for a flat bar; further, assuming the Tresca yield condition, the fully developed plastic moment is the same as for a flat bar.[70] As a result, it was decided this effect was not significant for the present work and no attempt was made to treat it for a more general plastic flow condition.

In the reverse bending experiments any residual stress retained in the bar from the previous run would influence the apparent initial flow stress. When a plastically bent bar is unloaded, a residual stress distribution results in the bar which is the difference between the non-linear stress distribution from bending and the linear elastic stress distribution of unloading.[70] Upon reloading in the opposite direction, the applied and residual stresses are additive so the total stress will be higher than the applied stress. This factor is not thought to be important in the present tests because of the rapid relaxation which occurs in the specimens after the test before cool down and during the hold time before the subsequent reloading. Qualitative support for this was obtained by the fact that if a test were terminated by stopping the cross-head, but not unloading, the load would relax to a small fraction of its initial value within about 10 minutes.

For some of the specimens subjected to multiple bending a considerable amount of strain enhanced grain growth occurred, resulting in a variation in grain size through the cross-section (see Figure 3). Since the flow stress increases rapidly with grain size, this produces an apparent strain hardening. The fact that the grain growth appears to be caused in part by direct thermal exposure and additionally as a result of strain leads to errors in the use of equations (A1) and (A2). The grain size variation in the sample leads to a change in the stress distribution in the bar; from an analytical point of view, this is not essentially different than other forms of strain hardening and the use of the proper value of n_b would account for it. Difficulty arises from the fact that the n_b determined experimentally will also reflect the time dependent grain growth; this does not cause a change in the shape of the stress distribution curve and so the n_b used in equation A1 should be reduced to eliminate the time dependent grain growth contribution or else the outer fiber stress will be over-estimated. A similar correction is required for the value of m_b determined experimentally since the apparent strain rate dependence determined at a constant value of strain will reflect time dependent differences; this will cause m_b to be lower, since the time dependent hardening will be greater at slower rates. A continuous separation of the time dependent and strain dependent grain growth throughout a test would be at best a difficult task. The net result is that a derived stress-strain curve would contain some direct error in the stress calculation and would, in addition, indicate hardening as a function of strain, whereas, it should in part be considered as only a coincident function of time.

B. Bending Moment Determination

It has been shown that at large deflections several of the assumptions of simple beam theory break down and several non-linear effects become significant. This problem has been recently treated for four-point elastic bending of thin beams;[71,72] several factors were identified which are also important in plastic bending to the large deflections used here (i.e., outer

fiber strains of ~5%). At large deflections the horizontal load component at the support becomes significant and substantially influences the applied bending moment. If the load points are not sharp knife edges, the actual point of tangency to the supports will shift during the test causing a continuous change in the moment arm and specimen length.

For bending a flat specimen the bending moment is given by the expression:

$$M_S = \frac{Pa}{2} \tag{A3}$$

where P is the total applied load and a is the moment arm. When the deflections become significant, however, the affect of the horizontal components on the moment must be considered. The horizontal forces are determined by the slope of the beam at the support as well as the friction at the knife edge. For the present case the thickness of the beam must also be considered, since it is significant with respect to the total deflections; this is in contrast to the elastic case where large deflections are obtained only in thin beams. From the force equilibrium equations the expression for the bending moment in the gage section is given by:

$$M = \frac{Pa}{2} + \frac{P}{2}\left(\frac{\sin\psi_1 - \mu\cos\psi_1}{\cos\psi_1 + \mu\sin\psi_1}\right)\left(y - \frac{h}{2\cos\psi_1}\right) - \frac{P}{2}\left(\frac{\sin\psi_2 + \mu\cos\psi_2}{\cos\psi_2 - \mu\sin\psi_2}\right)\left(y - y_2 + \frac{h}{2\cos\psi_2}\right)$$

$$(0 \le x \le L/2 - a) \tag{A4}$$

where the applicable geometry is defined in Figure A1 and μ is the coefficient of friction between the load supports and the specimen. For comparative purposes the ratio of the bending moment to that calculated neglecting curvature, M_S, is given by:

$$\frac{M}{M_S} = 1 + \frac{1}{a}\left(\frac{\sin\psi_1 - \mu\cos\psi_1}{\cos\psi_1 + \mu\sin\psi_1}\right)\left(y - \frac{h}{2\cos\psi_1}\right) - \frac{1}{a}\left(\frac{\sin\psi_2 + \mu\cos\psi_2}{\cos\psi_2 - \mu\sin\psi_2}\right)\left(y - y_2 + \frac{h}{2\cos\psi_2}\right)$$

$$(0 \le x \le L/2 - a) \tag{A5}$$

For the case of unbending a bent bar the applicable relation is:

$$\frac{M}{M_S} = 1 + \frac{1}{a}\left(\frac{\sin\psi_1 - \mu\cos\psi_1}{\cos\psi_1 + \mu\sin\psi_1}\right)\left(y + \frac{h}{2\cos\psi_1}\right) - \frac{1}{a}\left(\frac{\sin\psi_2 + \mu\cos\psi_2}{\cos\psi_2 - \mu\sin\psi_2}\right)\left(y - y_2 - \frac{h}{2\cos\psi_2}\right)$$

$$(0 \le x \le L/2 - a) \tag{A6}$$

Similar relations are also obtained to indicate the effect on the bending moment in the moment arm regions, for the cases of bending:

$$\frac{M}{M_S} = 1 + \frac{1}{L/2 - x}\left(\frac{\sin\psi_1 - \mu\cos\psi_1}{\cos\psi_1 + \mu\sin\psi_1}\right)\left(y - \frac{h}{2\cos\psi_1}\right)$$

$$(L/2 - a \le x \le L/2) \tag{A7}$$

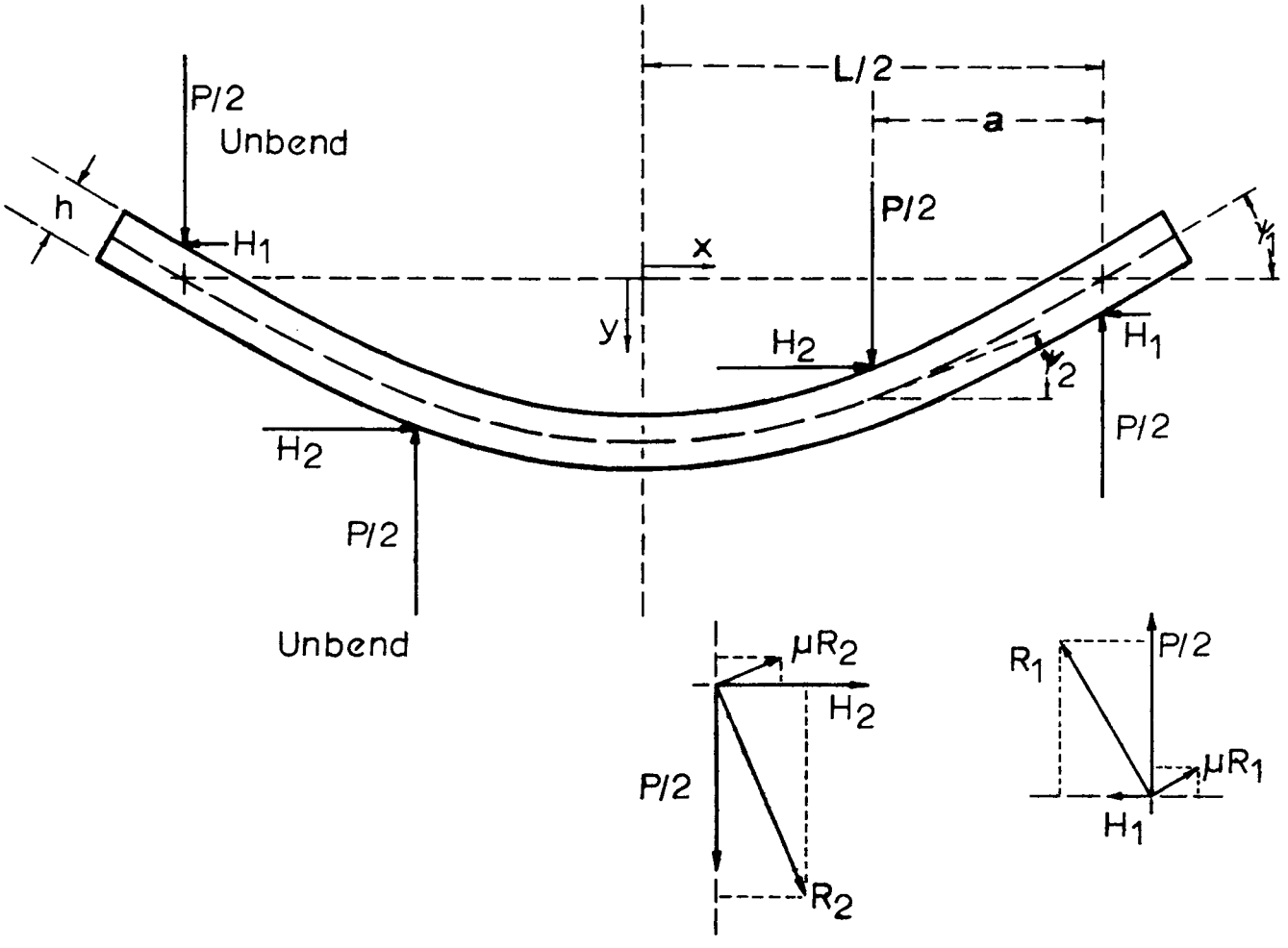

Figure A1. Schematic of Curved Bend Bar Showing Relevant Geometry; Resolution of the forces at the inner and outer supports is also shown.

and unbending:

$$\frac{M}{M_s} = 1 + \frac{1}{L/2 - x}\left(\frac{\sin\psi_1 - \mu\cos\psi_1}{\cos\psi_1 + \mu\sin\psi_1}\right)\left(y + \frac{h}{2\cos\psi_1}\right)$$

$$\left(L/2 - a \leq x \leq L/2\right) \qquad \text{(A8)}$$

In order to use these relationships for plastic bending, the values of x, y, ψ_1 and ψ_2 must be determined experimentally since they will vary somewhat for different constituitive relations. Further, these results are considerably influenced by the coefficient of friction, μ.

In order to indicate the magnitude of the effect, calculations of the M/M_S ratio were done for two situations and are presented in Table A1. The calculations for the large specimen were done with measurements from a bar strained to 4.2% on the first bend. The condition marked small bar is more representative of the values found in specimens after several rebends to nominal values in excess of 5% in which some non-uniformity occurred because of some hardening in the gage section (see text); this represents the most extreme condition utilized in this work. The ratio was calculated for the center of the gage section and for a point midway in the moment arm for each sample. It should be noted that the moment in the gage section is no longer constant under these conditions; it was shown, however, for the elastic case[71,72] that the variation in the gage section was only a couple of percent and the same condition should obtain for the plastic case. Inspection of equations (A5-A8) indicates that M/M_S approaches unity for flat bars.

Several interesting features can be seen from the table. The coefficient of friction has a strong influence on the actual moment as does the direction of bending. Estimation of the friction is difficult and it is likely that it fluctuates during the course of a test. It can be seen that for μ in excess of 0.5, the moment in the gage section decreases rapidly during bending and increased deflection in the moment arms is expected. This condition was not seen except in some bars after many bends for which there was reason to expect effective hardening of the gage section. It seems quite unlikely that the friction would be negligible. Therefore, a best estimate of the coefficient of friction is probably in the range of 0.2 to 0.5. It is seen that at these friction levels, the moment in rebending is initially in excess of that predicted by the simple calculation and the moment at the end of a run is less than that predicted by the simple theory. This effect would then account at least in part for the reduced initial loads seen on rebending specimens (see Figure 1).

The effect of shifting of the point of load contact was not included in the above results. The effect on the actual values of L and a are given by

$$L = L_o - 2R_1 \sin \psi_1 \qquad \text{(A9)}$$

$$a = a_o - R_1 \sin \psi_1 - R_2 \sin \psi_2$$

where R_1 and R_2 are the radii of curvature of the outer and inner knife edge load supports. During bending, a becomes smaller thereby raising the load and on unbending it is larger thus reducing the loads. This effect further accentuates the differences in loads required to bend and unbend. For the larger specimens R_1 and R_2 were about .008 inch so that the effect was small; for the smaller bars R_1 and R_2 were estimated to be about 0.015 inch so that the effect was appreciable; these results are also shown in Table A1.

As a result of the several necessary corrections and the uncertainties about several factors such as the coefficient of friction and grain growth effects, it was concluded that an attempt to quantitatively reduce all of the multiple bend tests was not warranted. This conclusion found further support from the obvious uncertainties after several bends caused by the non-uniform bending of the bars. It is seen that the two bending moment corrections account for a considerable amount of the load increase which occurred within each cycle and for the reduced load required to rebend. This analysis does, however, indicate that at the midpoint of a test when the bar was nearly flat, the simply calculated moment arm should be nearly correct. Therefore, for these specimens the moment was calculated using equation (A3). The stresses were calculated using the simple elastic relation:

$$\sigma = \frac{6\,M}{bh^2} \tag{A10}$$

because of uncertainty about the appropriate values of n_b and m_b to use. Since the rate sensitivity remained high, presumably 0.6-0.7, and there was often some grain size gradient, this stress value is not greatly in error.

For the change in rate tests, the total strains were held to less than 3% for most specimens in order to minimize the contributions from horizontal loading effects. These tests were done with large bars so the tangency shift was small. Since most samples give no evidence of a real hardening at these strains, n_b was assumed zero for analysis of these data; this made the data reduction comparable to previous work[25] with which they were being compared. The measured values of m_b were used to calculate the stresses.

C. Determinational Strain and Strain Rate

Strain is measured by the use of probes running directly to the specimen or to the specimen and load block. The deflection is measured with an LVDT and recorded continuously. For the most part, deflection of the specimen with respectto the inner knife edges was measured. Strain is then determined from the relation:

$$G = \frac{4\,hD}{l^2 + 4hD} \simeq \frac{4\,hD}{l^2} \tag{A11}$$

where D is the gage section deflection and l is the gage length. The previous analysis indicated that the bending moment remains nearly constant in the gage section so that this relation, which assumes only that pure bending occurs, remains valid for the conditions of these tests.

The strain rate is determined from the deflection versus time curves. Inspection of these curves indicated that it usually remains quite constant during the course of a test. In the multiple bending experiments the strain rate variations were seen to become more severe in successive tests. This is thought to be, in part, a result of hardening of the gage section which resulted in increased deflection occurring in the moment arms. In addition, variation in knife edge friction probably causes some fluctuation of the strain rate. It can be seen in Table A1 that as the friction increases the moment in the gage length is decreased faster than in the moment arms so that increases in knife edge friction would increase the strain in the moment arms and reduce the strain rate in the gage section.

The shift in point of tangency should cause a systematic increase in strain rate during the course of a test as a result of reduction in the value of a. In the multiple bend tests done with the small samples, where this effect was not negligible, the other variations often obscured this effect, particularly in the later cycles. For the large samples, this effect was very small.

TABLE A1

EFFECT OF CURVATURE ON THE BENDING MOMENT

Ratio of the Corrected to Simple Bending Moments, M/M_s.

Effect of Horizontal Loads.

Coefficient of Friction	Condition	Large Specimen at ϵ = 4.2%, $\psi_1 = 30^\circ$ Gage*	Mom. Arm*	Small Specimen at $\epsilon \approx 5$ +%, $\psi_1 = 40^\circ$ Gage	Mom. Arm
$\mu = 0$	Bend	1.179	1.129	1.579	1.514
	Unbend	1.451	1.496	2.009	2.097
$\mu = 0.3$	Bend	0.893	1.053	1.110	1.264
	Unbend	1.166	1.202	1.483	1.564
$\mu = 0.5$	Bend	0.713	1.013	0.841	1.203
	Unbend	1.017	1.050	1.328	1.433
$\mu = 1.0$	Bend	0.231	0.939	-0.067	0.947
	Unbend	0.722	0.766	0.712	0.886
	Shift of Point of Tangency				
	Bend	.982	.978	0.915	0.898
	Unbend	1.018	1.022	1.083	1.104

*Gage, $\chi = 0$; Moment Arm, $\chi = L/2 - a/2$.

VII. REFERENCES

1. a. R.W. Rice, "Hot Working Oxides," submitted for Refractory Oxides, ed. A. Alper, to be published by Academic Press.

   b. R.W. Rice, "Hot Forming of Ceramics," in Ultrafine-Grain Ceramics, ed. J.J. Burke, N.L. Reed, R. Weiss, Syracuse U. Press, (1970).

2. a. A.H. Heuer, W.H. Rhodes, D.J. Sellers and T. Vasilos, "Microstructure Studies of Polycrystalline Refractory Oxides," Avco Corp., Summary Report, Contract NOw-66-0506-(d), (1967).

   b. W.H. Rhodes, D.J. Sellers, T. Vasilos, A.H. Heuer, R.H. Duff and P. Burnett, Avco Corp., Summary Report, Contract NOw-65-0316-f (1966).

   c. L.A. Brissette, P. Burnett, R.M. Spriggs and T. Vasilos, J. Amer. Ceram. Soc., 49, 165 (1966).

3. W.H. Rhodes, D.J. Sellers, R.M. Cannon, A.H. Heuer, W.R. Mitchell and P. Burnett, "Microstructure Studies in Polycrystalline Refractory Oxides," Avco Corp., Summary Report, Contract N000-19-67-C-0336 (1968).

4. a. R.W. Rice and J.G. Hunt, "Semi-Continuous Pressure Sintering," Report for Contract NOw65-0382-C (1966).

   b. M.W. Benecke, "Semi-Continuous Pressure Sintering," Boeing Co., Final Report, Contract N00019-68-C-0165 (1969).

5. H.M. Harris, J.E. Kelley, P.H. Sunset and H.J. Kelly, "Hot Rolling of Oxide-Glass Compositions," Bureau of Mines Investigation 6967, (1967).

6. R.T. Dolloff and H.B. Probst, "Hot Extrusion of Carbides," presented at the 70th Annual Meeting of the Am. Ceram. Soc., April 1968. Am. Ceram. Soc. Bull., 47, (4), 441 (1968).

7. A. Accary, P. Magnier and M. Marchal, "Comportemant Méchanique a Haute Température Des Alliages U-C De Composition Proche De Celle Du Monocarbure Et Mise En Forme De Ces Alliages Par Extrusion," C.E.A., Direction Des Piles Atomiques, DM/1450, (May 1965).

8. W.H. Rhodes, D.J. Sellers, A.H. Heuer and T. Vasilos, "Development and Evaluation of Transparent Aluminum Oxide," Final Report, Contract N178-8986 (1 June 1966 - 30 June 1967).

9. R.M. Haag, "Magnetic-Crystallographic Orientation Produced in Ferrites by Hot-Working," Avco Corp., Contract N00014-68-C-0364, Annual Reports (March 1969 and March 1970).

VII. REFERENCES (Cont'd)

10. A.H. Heuer, D.J. Sellers and W.H. Rhodes, J. Am. Ceram. Soc., 52, 468 (1969).

11. R.B. Day and R.J. Stokes, J. Am. Ceram. Soc., 49, 345 (1966).

12. S.M. Copley and J.A. Pask, J. Am. Ceram. Soc., 48, 636 (1965).

13. H. Tagai and T. Zisner, J. Am. Ceram. Soc., 51, 303 (1968).

14. G.W. Groves and A. Kelly, Phil. Mag., 8, (89), 877 (1963).

15. R.C. Gifkins, "Intergranular Creep Fracture," Tewksbury Symposium on Fracture (1963), University of Melbourne, (1965).

16. R.B. Day and R.J. Stokes, J. Am. Ceram. Soc., 47, 493 (1964).

17. A.W. Mullendore and N.J. Grant, "Grain Boundary Behavior in High Temperature Deformation," Proceedings of the 8th Sagamore Ordnance Materials Research Conference, The Ordnance Materials Research Office, (1961).

18. E.M. Passmore, R.H. Duff and T. Vasilos, J. Am. Ceram. Soc., 49, 594 (1966).

19. R.W. Rice, J. Am. Ceram. Soc., 52, 428 (1969).

20. J.W. Cahn, Acta. Met., 10, 789 (1962).

21. D.M. Choi and H. Palmour III, "Flow and Fracture of Hot Pressed Polycrystalline Spinel at Elevated Temperatures," North Carolina State University, Technical Report, Contract DA-31-124-ARO-D-207 (August 1965).

22. L.E. Poteat and C.S. Yust, "Grain Boundary Reactions During Deformation in Ceramic Microstructures," ed. R.M. Fulrath and J.A. Pask, Wiley (1968).

23. J.S. Nadeau, J. Am. Ceram. Soc., 52, 1 (1969).

24. W.L. Barmore and R.R. Vandervoort, J. Am. Ceram. Soc., 50, 316 (1967).

25. A.H. Heuer, R.M. Cannon and N.J. Tighe, "Plastic Deformation in Fine-Grain Ceramics," in Ultrafine-Grain Ceramics, ed. J.J. Burke, N.L. Reed, R. Weiss, Syracuse Univ. Press, (1970).

26. E. Stofel and H. Conrad, Trans. AIME, 227, 1053 (1963).

27. P.F. Becher and H. Palmour III, J. Am. Ceram. Soc., 53, 119 (1970).

VII. REFERENCES (Cont'd)

28. G.W. Groves and A. Kelly, Phil. Mag., 19, 977 (1967).

29. R.C. Folweiler, J. Appl. Phys., 32, 773 (1961).

30. S.I. Warshaw and F.H. Norton, J. Am. Ceram. Soc., 45, 479 (1962).

31. W.L. Barmore and R.R. Vandervoort, J. Am. Ceram. Soc., 48, 499 (1965).

32. C. Herring, J. Appl. Phys., 21, 437 (1950).

33. R.L. Coble, J. Appl. Phys., 34, 1679 (1963).

34. I.M. Litshitz, Soviet Phys. JETP, 17, 909 (1963).

35. W.M. Armstrong, W.R. Irvine and R.H. Martison, J. Nucl. Matl's., 7, 133 (1962).

36. L.E. Poteat and C.S. Yust, J. Am. Ceram. Soc., 49, 410 (1966).

37. P.E. Bohaboy and S.K. Evans, presented 72nd Am. Ceram. Soc. Meeting, Am. Ceram. Soc. Bull., 49, 445 (1970).

38. T.G. Langdon and J.A. Pask, Acta.Met., 18, 505 (1970).

39. C.A.P. Horton and C.J. Beevers, Acta. Met., 16, 733 (1968).

40. H. Gleiter, E. Hornbogen and G. Baro, Acta. Met., 16, 1053 (1968).

41. T.H. Alden, Trans. ASM, 61, 559 (1968).

42. A. Ball and M.M. Hutchison, Met. Sci. J., 3, 1 (1969).

43. R.E. Fryxell and B.A. Chandler, J. Am. Ceram. Soc., 47, 283 (1964).

44. E.M. Passmore and T. Vasilos, J. Am. Ceram. Soc., 49, 166 (1966).

45. R. Scott, A.R. Hall and J. Williams, J. Nucl. Matl's., 1, 39 (1959).

46. W.M. Armstrong, W.R. Irvine, J. Nucl. Matl's., 9, 121 (1963).

47. a. G.T. Murray, J. Silgailis and A.J. Mountvala, J. Am. Ceram. Soc., 47, 531 (1964).

    b. M.A. Adams and G.T. Murray, J. Appl. Phys., 33, 2126 (1962).

48. J. Intrater and E.S. Machlin, Acta. Met., 7, 140 (1959).

VII. REFERENCES (Cont'd)

49. H. Brunner and N.J. Grant, Trans. AIME, 215, 48 (1959).

50. E.W. Hart, Acta. Met., 15, 351 (1967).

51. R.M. Spriggs, L.A. Brissette and T. Vasilos, J. Am. Ceram. Soc., 47, 417 (1964).

52. D.V. Poluboyarinov, R. Ya. Popil'skii, I.P. Galkina and V.S. Bakunou, Izv. Akad. Nauk. SSSR, Neorg. Mat'l., 2, 1115 (1966).

53. W.H. Rhodes and R.M. Cannon, "Microstructure Studies of Refractory Polycrystalline Oxides," Summary Report, Avco Corp., Contract N00019-69-C-0198, (1969).

54. A.M. Sabroff, F.W. Boulger and H.J. Henning, Forging Materials and Practices, Reinhold, New York, p. 50, (1968).

55. W.H. Rhodes, P.F. Jahn and P.L. Burnett, Microstructural Studies of Polycrystalline Oxides, Summary Report, Contract N00019-68-C-0108, (25 May 1968 - 24 June 1969).

56. C.S. Barrett and T.B. Massalski, Structure of Metals, 3rd ed., McGraw-Hill, New York (1966).

57. M.L. Kronberg, J. Am. Ceram. Soc., 45, 274 (1962).

58. H. Conrad, G. Stone and K. Janowski, Trans. AIME, 233, 89 (1965).

59. H. Palmour III, et al, "Grain Boundary Sliding in Alumina Bicrystals," North Carolina State U., Progress Report No. ORO-3328-9, Contract AT-(40-1)-3328 (December 1968).

60. P.D. Bayer and R.E. Cooper, J. Mat'l. Sci., 2, 301 (1967).

61. T.D. Gulden, J. Am. Ceram. Soc., 50, 472 (1967).

62. C.A. May and K.H.G. Ashbee, Micron, 1, 62 (1969).

63. H. Conrad, J. Am. Ceram. Soc., 48, 195 (1965).

64. J.C.M. Li, J. Appl. Phys., 32, 593 (1961).

65. C. Crussard and J. Friedel, "Theory of Accelerated Creep and Rupture," in Creep and Fracture of Metals at High Temperatures, NPL Symposium, HMSO, p. 243 (1956).

66. W.D. Scott and J.A. Pask, J. Am. Ceram. Soc., 46, 284 (1963).

67. R.L. Coble and Y.H. Guerard, J. Am. Ceram. Soc., 46, 353 (1963).

VII. REFERENCES (Concl'd)

68. N.J. Grant and A.R. Chaudhuri, "Creep and Fracture," in Creep and Rupture, ASM, Cleveland (1957).

69. A.H. Heuer and R.M. Cannon, Jr., "Plastic Deformation of Fine Grained Aluminum Oxide," presented at Symposium on Mechanical Testing Procedures for Brittle Materials, March 28-30, 1967, IITRI, Chicago, Ill.

70. W. Johnson and P.B. Meller, Plasticity for Mechanical Engineers, D. Van Nostrand, London, p. 98, 111 (1962).

71. R.D. Schile and R.L. Sierakowski, Int. J. Non-Linear Mech., 2, 61 (1967).

72. D.L. Vrooman and J.E. Ritter, Jr., Am. Ceram. Soc. Bull., 49, 789 (1970).